

Colloquium: Nonlinear Collective Interactions in Dense Plasmas

P. K. Shukla and B. Eliasson

*Fakultät für Physik und Astronomie, Ruhr-Universität Bochum, D-44780 Bochum, Germany**

(Received 27 September 2010)

The current understanding of some important collective processes in dense quantum plasmas is presented. After reviewing the basic properties of dense quantum plasmas with degenerate electrons, we present model equations (e.g. the quantum hydrodynamic and effective nonlinear Schrödinger-Poisson equations) that describe collective nonlinear phenomena at nanoscales. The effects of the electron degeneracy arise due to Heisenberg's uncertainty principle and Pauli's exclusion principle for overlapping electron wave functions that result in a nonlinear quantum electron pressure and tunneling/diffusion of electrons through a nonlinear quantum Bohm potential. Since degenerate electrons have $1/2$ -spin due to their Fermionic nature, there also appear a spin electron current and a spin force acting on the electrons due to the Bohr magnetization. The present nonlinear equations do not include strong electron correlations and electron-exchange interactions. The quantum effects caused by the electron degeneracy produce new aspects of electrostatic and electromagnetic oscillations in dense quantum plasmas that are summarized in here. Furthermore, we shall discuss nonlinear features of electrostatic ion and Langmuir waves, as well as trapping of intense electromagnetic waves in density holes. Specifically, simulation studies of the nonlinear Schrödinger (NLS) and Poisson equations reveal the formation and dynamics of localized electrostatic structures at nanoscales in dense quantum plasmas. We also discuss the effect of an external magnetic field on the plasma wave spectra and develop the quantum magnetohydrodynamic equations in dense quantum magnetoplasmas. The results of our investigation are useful for understanding numerous collective processes (e.g. the plasma wave spectra and the associated localization of the wave energy) in degenerate plasmas, such as those in compact astrophysical objects (e.g. the cores of white dwarf stars and giant planets), as well as in plasma-assisted nanotechnology (e.g. quantum diodes, quantum free-electron lasers, nanophotonics and nanoplasmonics, metallic nanostructures, thin metal films, semiconductor quantum wells and quantum dots, etc.), and in the next-generation intense laser-solid density plasma interaction experiments relevant for fast ignition in inertial confinement fusion schemes.

PACS numbers: 05.30.Fk, 52.35.Mw, 52.35.Ra, 52.35.Sb

Contents		B. Nonlinearly Coupled Intense EM and EPOs	16
I. Introduction	1	VIII. Dense magnetized Plasmas	18
II. Basic Properties of Quantum Plasmas	4	A. Landau Quantization	18
III. Model Equations for Quantum Systems	5	B. ESOs and EM Waves	19
A. The Klein-Gordon Equation	5	C. Q-HMHD Equations	20
B. The Dirac and Pauli Equations	5	IX. Summary and Outlook	20
C. The Schrödinger and Wigner-Poisson Equations	7	Acknowledgments	21
D. The QHD Equations	8	References	21
E. The NLS-Poisson Equations	8		
IV. Linear Waves in Quantum Plasmas	8		
V. Quantum Dark Solitons and Vortices	10	I. INTRODUCTION	
A. Quantum Electron Holes	11		
B. Quantum Electron Vortices	11		
VI. Quantum Electron Fluid Turbulence	12		
A. Modeling Methods and Plasma Parameters	13		
B. Formation of Quantum Structures and Associated Spectra	13		
VII. Nonlinearly Coupled Electromagnetic and Electrostatic Waves	15		
A. Stimulated Scattering Instabilities	15		

Very dense plasmas composed of degenerate electrons, positrons, and holes are referred to as quantum plasmas. In the latter, the degeneracy of the plasma particles appears at very high densities, where inter-plasma particle distance is of the order of the de Broglie thermal wavelength or even comparable with the Compton length. In such a situation, Heisenberg's uncertainty principle (Bransden, 2000; Dirac, 1981; Holland, 1993; Landau and Lifshitz, 1998a) dictates that the position and momentum of charged particle (e.g. electrons, positrons) cannot be precisely determined simultaneously; the product of the uncertainties of the position and momentum is

*Electronic address: profshukla@yahoo.com; beliass@yahoo.se

greater than $\hbar/2$, where \hbar is the Planck constant divided by 2π . The position of an electron subjected to the influence of an atomic nucleus is very well defined (the force to which it is subjected is large). However, owing to Heisenberg's uncertainty principle, the electron momentum is ill defined. An electron has a continuous motion around the position it occupies. This motion exerts pressure on the surrounding medium, exactly as the thermal agitation of the particles of a gas exerts its pressure. This pressure is called the pressure of electron degeneracy. This pressure, since it is nonthermal in origin, is, of course, independent of the electron temperature; the pressure of the degenerate electrons increases with increasing electron number density. It is, however, only at very high densities that the degeneracy pressure becomes comparable or larger to the thermal gas pressure. We then say that the plasma matter is in an exotic state, comprising degenerate electrons and positrons/holes.

Let us suppose that dense quantum plasmas are composed of degenerate electrons of mass m_e and number density n_e , and the ions of mass m_i and number density n_i . The ions are typically non-degenerate, because they are much heavier in comparison with the electrons. Each electron will on average occupy a volume $1/n_e$. Then, by Heisenberg's uncertainty principle (Bransden, 2000), $\Delta x \Delta p \approx \hbar/2$, the momentum of the electron will be $p_x \approx \hbar n_e^{1/3}$. If the electrons are non-relativistic, the velocity of the electron will be $\sim p_x/m_e = \hbar n_e^{1/3}/m_e$; however, if the electrons are relativistic, their velocity will be close to c , the speed of light in vacuum. Now the electron pressure, as it is for a simple gas, is the momentum transfer per unit area, or $P_e = \text{momentum} \times (\text{velocity}) \times (\text{number density})$. For non-relativistic electrons, we have (Gursky, 1976) $P_e = \hbar n_e^{1/3} (\hbar n_e^{1/3}/m_e) n_e = \hbar^2 n_e^{5/3}/m_e$. On the other hand, when the electrons are relativistic, the relativistic electron pressure is $P_{er} = \hbar n_e^{1/3} c n_e = \hbar c n_e^{4/3}$. In the past, Chandrasekhar (1931, 1935, 1939) presented a rigorous derivation of the electron pressure P_C for arbitrary electron degeneracy in dense matters with a Fermi-Dirac electron distribution function. It reads

$$P_C = \frac{\pi}{3h^3} m_e^4 c^5 f(\xi_c), \quad (1)$$

where $f(\xi_c) = \xi_c(2\xi_c^2 - 3)(1 + \xi_c^2)^{1/2} + 3\sinh^{-1}(\xi_c)$, $\xi_c = p_c c/m_e c$, and $p_c = (3h^3 n_e/8\pi)^{1/3}$ is the momentum of an electron on the Fermi surface. In the non-relativistic limit $\xi_c \rightarrow 0$, we have (Chandrasekhar, 1935, 1939)

$$P_n = \frac{(\pi)^{2/3}}{5m_e} \hbar^2 n_e^{5/3}, \quad (2)$$

while in the ultra-relativistic limit $\xi_c \rightarrow \infty$, Chandrasekhar's degenerate electron pressure reads (Chandrasekhar, 1931)

$$P_u = \frac{(3\pi^2)^{1/3}}{4} \hbar c n_e^{4/3}. \quad (3)$$

Thus, the intuitively obtained formulas of Gursky (1976) for the non-relativistic and ultra-relativistic pressures for degenerate electrons are in agreement with those deduced from Chandrasekhar's pressure formula (Chandrasekhar, 1935, 1939) for an arbitrary electron degeneracy.

In his Nobel Prize winning paper, Chandrasekhar (1931) had balanced the gradient of the ultra-relativistic generate electron pressure P_c/R and the gravitational force $G = (GM/R^2)n_e m_n$, where G is the gravitational constant, M and R are the mass and radius of a star, respectively, m_n the mass of nuclei ($n_e m_n = M/R^3$), to deduce the critical mass of a star $M_c = (\hbar c/G)^{3/2} m_n^{-2} \approx 1.4M_s$, where M_s is the solar mass. Since M_c is independent of density, it means that this mass is obtained independent of radius. This is the limiting mass; more massive stars cannot be supported by electron degeneracy pressure no matter how small they are. This was the discovery of Chandrasekhar; that the pressure dependence on density changed in going from nonrelativistic to relativistic conditions and, as a consequence, there arose a finite limit to the mass of a star with ultra-relativistic degenerate electrons. Relativistic degenerate electrons are found in the core of massive white dwarf stars (Koester and G. Chanmugam, 1990; Shapiro, 1983), aptly named due to their very low luminosities yet high surface emissivities, are compact bodies with radii $\leq 10^{-2}R_s$ and masses typically $\leq M_s$. Consequently, the average electron number densities are quite high ($\sim 10^{30} \text{ cm}^{-3}$).

The Fermi dense plasma with degenerate electrons and positrons falls under the category of extreme states of matter (Fortov, 2009; Ichimaru, 1982) (densities comparable with solids and temperatures of several electron volts) that appear in the core of giant planets (Chabrier *et al.*, 2006; Chabrier, 2009; Horn, 1991) and the crusts of old stars (Guillot, 1999). Dense compressed plasmas are currently of wide interest due to their applications to astrophysical and cosmological environments (Benvenuto and De Vito, 2005; Harding and Lai, 2006; Lai, 2001; Opher, 2001), as well as to inertial fusion science involving intense laser-solid density plasma interaction experiments (Andreev, 2000; Glenzer and Redmer, 2009; Glenzer *et al.*, 2007; Hu and Keitel, 1999; Kritcher *et al.*, 2008; Lee *et al.*, 2009; Malkin *et al.*, 2007; Marklund and Shukla, 2006; Mendonça, 2001; Neumayer *et al.*, 2010; Salamin *et al.*, 2006; Son and Fisch, 2004) for inertial confinement fusion (Azechi *et al.*, 2006) based on the high-energy density plasma physics (Drake, 2009; Norreys *et al.*, 2009). Furthermore, due to recent experimental progress in femtosecond pump-probe spectroscopy, the field of dense quantum plasmas is also gaining significant attention (Crouseilles *et al.*, 2008) in connection with the collective dynamics of an ensemble of degenerate electrons in metallic nanostructures, and in thin metal films. The physics of quantum plasmas is also relevant in the context of quantum diodes (Ang *et al.*, 2003, 2007; Shukla and Eliasson, 2008b), nanophotonics and nanowires (Barnes *et al.*, 2003; Chang *et al.*, 2006; Shpatakovskaya, 2006), nanoplasmonics (Atwater,

2007; Maier, 2007; Marklund *et al.*, 2008; Ozbay, 2006), high-gain quantum free-electron lasers (Serbeto *et al.*, 2008, 2009), microplasma systems (Becker *et al.*, 2006), and small semiconductor devices (Haug and Koch, 2004; Manfredi and Hervieux, 2007; Markovich *et al.*, 1990), such as quantum wells and quantum dots. The latter are relevant for quantum computing.

Collective interactions between an ensemble of degenerate electrons and positrons/holes give rise to novel waves and structures in dense quantum plasmas. Studies of linear waves in a non-relativistic unmagnetized quantum plasma with degenerate electrons begun with the pioneering theoretical works of Bohm (1953); Bohm and Pines (1953); Klimontovich and Silin (1952a,b, 1961), and Pines (1961), who studied the dispersion properties of the high-frequency electron plasma oscillations (EPOs). The frequencies of the latter with an arbitrary electron degeneracy were presented by Maafa (1993). In the theoretical description of the EPOs, Klimontovich-Silin and Bohm-Pines used the Wigner quantum distribution function (Wigner, 1932) and the density matrix approach to demonstrate that in a very dense quantum plasma with the Fermi-Dirac equilibrium distribution function for the degenerate electrons the frequency of the EPOs is significantly different from the Bohm-Gross frequency in a classical electron-ion plasma with non-degenerate electrons obeying the Boltzmann-Maxwell distribution function. The dispersion to the EPOs involving the quantum nature appears through the Fermi electron thermal speed and a quantum dispersion arising from a quantum mechanical diffusion and tunneling of the electrons through the quantum Bohm potential (Gardner and Ringhofer, 1996; Jungel *et al.*, 2006; Manfredi, 2005; Manfredi and Haas, 2001; Misra, 2009; Shukla, 2006; Shukla and Eliasson, 2006, 2010). The quantum Bohm potential first appeared in Madelung's quantum fluid description of a single electron (Madelung, 1926). The quantum forces in dense plasmas arise due to the overlapping of the electron wave functions, a phenomena described by Heisenberg's uncertainty principle in quantum mechanics. The quantum longitudinal and transverse dielectric constants of an isotropic plasma have also been worked out (Kuzelev and Rukhadze, 1999; Silin and Rukhadze, 1961). Contributions of the electron spin and electron exchange interactions to the electromagnetic wave dispersion relations in an unmagnetized quantum plasma have been presented by Burt and Wahlquist (1962). Oberman and Ron (1963) derived the expression for the dielectric function for longitudinal waves in a non-relativistic magnetized quantum plasma and discussed applications of their work to heavily doped semiconductors. Kelly (1964) studied the dispersive properties of a magnetized quantum plasma by using the Wigner function and the Maxwell equations. Furthermore, there are also some papers dealing with the high-frequency wave propagation (Hakim and Heyvaerts, 1978; Melrose, 2008), and wakefields (Zhu and Ji, 2010) in an unmagnetized quantum plasma with relativistic elec-

trons.

During the last decade, there has been a surge in investigating new aspects of collective interactions in dense quantum plasmas by developing non-relativistic quantum hydrodynamic (Gardner and Ringhofer, 1996; Jungel *et al.*, 2006; Manfredi, 2005; Manfredi and Haas, 2001; Shukla and Eliasson, 2010) and quantum kinetic (Bonitz, 1998; Kremp *et al.*, 1999, 2005; Tsintsadze and Tsintsadze, 2009) equations. The Wigner-Poisson (WP) model (Hillery *et al.*, 1984) has been used to derive a set of quantum hydrodynamic (QHD) equations (Manfredi, 2005; Manfredi and Haas, 2001) for electrostatic waves in a dense quantum plasma. The non-relativistic QHD equations include the continuity, momentum and Poisson equations. The quantum nature (Manfredi and Haas, 2001; Shukla and Eliasson, 2010) is manifested in the non-relativistic electron momentum equation through the quantum statistical pressure term, which requires the knowledge of the Wigner electron distribution function for a quantum mixture of electron wave functions, each characterized by an occupation probability. The quantum part of the electron pressure is also represented as a nonlinear quantum force (Gardner and Ringhofer, 1996; Manfredi and Haas, 2001) $-\nabla\phi_B$, where $\phi_B = -(\hbar^2/2m_e\sqrt{n_e})\nabla^2\sqrt{n_e}$. Defining the effective wave function $\psi = \sqrt{n_e(\mathbf{r}, t)} \exp[iS_e(\mathbf{r}, t)/\hbar]$, where $\nabla S_e(\mathbf{r}, t) = m_e \mathbf{u}_e(\mathbf{r}, t)$ and $\mathbf{u}_e(\mathbf{r}, t)$ is the electron velocity, the non-relativistic electron momentum equation can be cast as an effective nonlinear Schrödinger (NLS) equation (Manfredi, 2005; Manfredi and Haas, 2001; Shukla, 2006; Shukla and Eliasson, 2006, 2010), in which there appears a coupling between the electron wave function and the electrostatic potential associated with the EPOs. The electrostatic potential, in turn, is determined from Poisson's equation. One thus has the coupled NLS and Poisson equations, governing the dynamics of nonlinearly interacting EPOs in a very dense quantum plasma. Both the non-relativistic QHD equations and NLS-Poisson equations exclude strong interactions among the quantum particles and electron exchange interactions (Hohenberg and Kohn, 1964; Kohn and Sham, 1965) between an electron and the background plasma particles (e.g. degenerate electrons and non-degenerate ions). However, it has turned out that both the QHD and NLS-Poisson equations have been quite useful for studying linear and nonlinear plasma waves as well as stability of quantum plasmas (Haas, 2005, 2007; Haas *et al.*, 2003; Manfredi, 2005; Manfredi and Haas, 2001; Shukla, 2006; Shukla and Eliasson, 2006, 2010) at nanoscales involving different quantum forces (e.g. associated with the quantum Bohm potential (Gardner and Ringhofer, 1996) and the quantum pressure law (Manfredi, 2005; Manfredi and Haas, 2001; Shukla and Eliasson, 2010) for a degenerate quantum plasma. New effects also appear when one accounts for the potential energy of the electron $-1/2$ spin magnetic moment in a magnetic field (Brodin and Marklund, 2007a,b,c; Brodin *et al.*, 2008, 2010; Marklund and Brodin, 2007; Misra, 2007, 2009; Misra and Samanta,

2010; Shukla, 2007, 2009; Takabayashi, 1955)). In fact, the QHD model for the electrons in both non-relativistic (Manfredi, 2005; Manfredi and Haas, 2001; Shukla, 2006; Shukla and Eliasson, 2006, 2010) and ultra-relativistic (Chandrasekhar, 1931, 1939) quantum plasma regimes seem to provide an adequate description for probing some quantum collective interactions in compressed plasmas (Glenzer and Redmer, 2009; Glenzer *et al.*, 2007; Lee *et al.*, 2009; Neumayer *et al.*, 2010) due to the availability of ultrafast x-ray Thompson scattering spectroscopic techniques.

In this Colloquium, we present our current knowledge of numerous collective processes in dense quantum plasmas with degenerate electrons. To start with, we describe the salient properties of dense quantum plasmas in which the degenerate electrons follow the Fermi-Dirac distribution. We then continue presenting the relevant equations for treating the linear and nonlinear wave phenomena in our dense quantum plasma. After reviewing the linear properties of electrostatic and electromagnetic waves in quantum plasmas, we go on presenting numerical results of the governing nonlinear equations that reveal localization of electrostatic and electromagnetic waves at nanoscales. Specifically, we shall discuss the formation and dynamics of nanostructures (e.g. one-dimensional quantum electron density hole and two-dimensional quantum vortices), as well as dwell on the properties of the 3D quantum electron fluid turbulence at nanoscales. Also presented are the nonlinear interactions between intense electromagnetic waves and electrostatic oscillations, which reveal stimulated scattering of electromagnetic waves off plasma oscillations and trapping of light into a quantum electron hole in dense quantum plasmas. The effects of an external magnetic field on the linear and nonlinear wave phenomena in dense magnetoplasmas are examined. Finally, we shall highlight possible applications, as well as the future perspectives and outlook of the nonlinear quantum plasma physics.

II. BASIC PROPERTIES OF QUANTUM PLASMAS

Let us first summarize some of the basic properties of quantum plasmas that are quite distinct from classical plasmas. While classical plasmas are composed of non-degenerate plasma particles with low number densities and relatively high electron and ion temperatures, quantum plasmas have degenerate quantum particles (electrons, positrons, and holes) and the plasma particle number densities are extremely high. As the electron density increases, the electron Fermi energy is no longer negligible in comparison with the electron mass energy and the speed of an electron on the Fermi surface becomes comparable to the speed of light in vacuum. The parameter regimes (the electron temperature versus the electron number density) under which quantum plasmas occur are depicted in Fig. 1.

Quantum mechanical effects start playing a significant

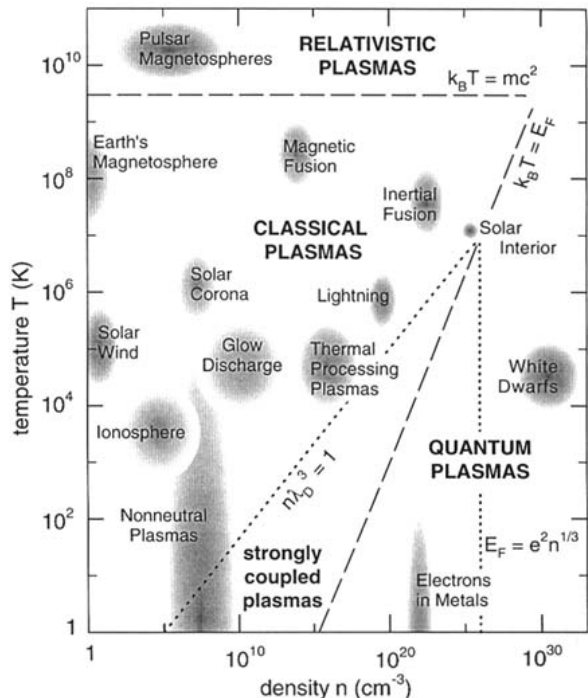


FIG. 1 The plasma diagram in the $\log T$ - $\log n_e$ plane, separating the classical and quantum regimes. After National Academic Press (1995).

role when the average inter-particle distance $d = n^{-1/3}$ is smaller (or even comparable) to the thermal de Broglie wavelength [$\lambda_B = \hbar/mV_T$, where m is the mass of the quantum particles (e.g. degenerate electrons, degenerate positrons, degenerate holes), $V_T = (k_B T/m)^{1/2}$ the thermal speed of the degenerate quantum particles having the temperature T and the mass m , and k_B the Boltzmann constant], i.e. when

$$n\lambda_B^3 \geq 1, \quad (4)$$

or, equivalently, the temperature is comparable or lower than the Fermi temperature $T_F = E_F/k_B$, where the Fermi energy of the degenerate quantum particle is

$$E_F = \frac{\hbar^2}{2m} (3\pi^2)^{2/3} n^{2/3}. \quad (5)$$

It then turns out that

$$\frac{T_F}{T} = \frac{1}{2} (3\pi^2)^{2/3} (n\lambda_B^3)^{2/3} \geq 1. \quad (6)$$

When the plasma particle temperature approaches T_F , one can show, by using density matrix formalism (Bransden, 2000), that the equilibrium distribution function changes from the Maxwell-Boltzmann $\propto \exp(-E/k_B T)$ to the Fermi-Dirac distribution function

$$F_D = \frac{2}{n_0} \left(\frac{m}{2\pi\hbar} \right)^3 [1 + \exp(E - \mu_j)/k_B T_F]^{-1}, \quad (7)$$

where in the non-relativistic limit the energy is $E = (m/2)v^2 = (m/2)(v_x^2 + v_y^2 + v_z^2)$. The chemical potential is denoted by μ_j , where the subscript j stands for the quantum particle species j . Accordingly, the equilibrium electron number density is

$$n_0 = -\frac{1}{4} \left(\frac{2mk_B T_F}{\pi \hbar} \right)^{3/2} \text{Li}_{3/2}[-\exp(\xi_\mu)], \quad (8)$$

where $\text{Li}_{3/2}$ is the poly-logarithm function, and $\xi_\mu = \mu_j/k_B T_F$.

It is useful to define the quantum coupling parameter Γ_Q , which is the ratio between the electrostatic interaction energy E_{int} between charged quantum particles (e.g. $E_{int} = 4\pi e^2 n^{1/3}$) and the Fermi thermal energy $E_F = k_B T_F$, where e is the magnitude of the electron charge. We have

$$\Gamma_Q = \frac{E_{int}}{E_F} \equiv \left(\frac{1}{n\lambda_F^3} \right)^{2/3} = 6\pi^2 \left(\frac{\hbar\omega_p}{k_B T_F} \right)^2, \quad (9)$$

where $\lambda_F = V_F/\omega_p$ is the Fermi screening radius, $V_F = (2E_F/m)^{1/2} = (\hbar/m)(3\pi^2 n)^{1/3}$ the Fermi thermal speed, and $\omega_p = (4\pi n e^2/m)^{1/2}$ the plasma frequency.

III. MODEL EQUATIONS FOR QUANTUM SYSTEMS

The solutions of the Klein-Gordon, Dirac, and Maxwell equations shall provide a very useful tool for studying the physics of a relativistic quantum particles (e.g. electrons and positrons) when the medium is driven by intense electromagnetic fields.

A. The Klein-Gordon Equation

Historically, the Klein-Gordon (KG) equation for an electron is obtained from the relativistic relation between the energy \mathcal{E}_e and the momentum \mathbf{p}_e

$$\mathcal{E}_e^2 = p_e^2 c^2 + m_e^2 c^4, \quad (10)$$

where \mathbf{p}_e is the electron momentum. By using the eikonal representation, viz. $\mathcal{E}_e \rightarrow i\hbar\partial/\partial t$ and $\mathbf{p}_e = -i\hbar\nabla$, we obtain from (10) the KG equation for a free electron as

$$\frac{\partial^2 \psi}{\partial t^2} - c^2 \nabla^2 + K_e^2 \psi = 0, \quad (11)$$

where $\psi(\mathbf{r}, t)$ is the electron wave function, and $K_e = m_e c/\hbar$. The quantum-particle KG equation satisfies the continuity equation

$$\frac{\partial \rho_e}{\partial t} + \nabla \cdot \mathbf{j}_e = 0, \quad (12)$$

where the electric charge and electric current densities are, respectively,

$$e\rho_e(\mathbf{r}, t) = -\frac{ie\hbar}{2m_e c^2} \left(\psi^* \frac{\partial \psi}{\partial t} - \psi \frac{\partial \psi^*}{\partial t} \right), \quad (13)$$

and

$$e\mathbf{j}_e(\mathbf{r}, t) = \frac{ie\hbar}{2m_e} (\psi^* \nabla \psi - \psi \nabla \psi^*). \quad (14)$$

In the presence of the self-consistent scalar and vector potentials ϕ and \mathbf{A} , respectively, one can cast the KG equation as

$$\mathcal{W}^2 \psi - c^2 \mathcal{P}^2 \psi - m_e^2 c^4 \psi = 0, \quad (15)$$

where we have defined the energy and momentum operators as

$$\mathcal{W} = i\hbar \frac{\partial}{\partial t} + e\phi, \quad (16)$$

and

$$\mathcal{P} = -i\hbar \nabla + e\mathbf{A}. \quad (17)$$

The electric charge and electric current densities of electrons, for our purposes, are, respectively,

$$e\rho_e = -\frac{ie\hbar}{2m_e c^2} (\psi^* \mathcal{W} \psi + \psi \mathcal{W} \psi^*), \quad (18)$$

and

$$e\mathbf{j}_e = \frac{ie\hbar}{2m_e} (\psi^* \mathcal{P} \psi + \psi \mathcal{P} \psi^*). \quad (19)$$

The charge and current densities here also obey the continuity equation.

The self-consistent vector and scalar potentials are obtained from the Maxwell-Poisson equations, yielding

$$\frac{\partial^2 \mathbf{A}}{\partial t^2} + c^2 \nabla \times (\nabla \times \mathbf{A}) + c \nabla \frac{\partial \phi}{\partial t} = 4\pi c \mathbf{j}_e, \quad (20)$$

and

$$\nabla^2 \phi + \frac{1}{c} \nabla \cdot \frac{\partial \mathbf{A}}{\partial t} = 4\pi(\rho_e + \rho_i), \quad (21)$$

where $\rho_i = en_0$ is the neutralizing positive charge density of ions. The electric ion current density is much smaller (by a factor of the electron to ion mass ratio) in comparison with \mathbf{j}_e , and has been neglected here. Equations (20) and (21) are useful for studying the nonlinear propagation of electromagnetic waves in a quantum system.

B. The Dirac and Pauli Equations

In relativistic quantum mechanics, the Dirac equation is capable of connecting quantum mechanics with special relativity. The quantum particles have spin. An electron spin $s = 1/2$ is an intrinsic property of electrons which have intrinsic angular momentum characterized by quantum number $1/2$, and a magnetic moment by individual electrons. Classically this would occur if the electron were spinning ball of charge, and this property was called

electron spin. In fact, the Dirac equation provides a description of the spin of the quantum particles. The spin of the electron (and positron)-which have the spin-1/2-is introduced through Dirac's Hamiltonian

$$\mathcal{H} = c\boldsymbol{\alpha}_s \cdot (\mathbf{p}_e + \frac{e}{c}\mathbf{A}) - e\phi + \beta m_e c^2, \quad (22)$$

where $\mathbf{p}_e = -i\hbar\nabla$ is the momentum operator, $\boldsymbol{\alpha}_s$ and β are the Dirac matrices. The three Cartesian components α_j ($j = 1, 2, 3$) of $\boldsymbol{\alpha}_s$ are usually constructed with help of the Pauli spin matrices σ_x , σ_y and σ_z (Bransden, 2000). The corresponding wave functions ψ are four-component spinors. A non-relativistic Dirac's Hamiltonian (associated with the Pauli equation) for the electrons is of the form

$$\mathcal{H} = -\frac{1}{2m_e} \left(\mathbf{p}_e + \frac{e}{c}\mathbf{A} \right)^2 + \mu_B \mathbf{B} \cdot \boldsymbol{\sigma} - e\phi, \quad (23)$$

where $\mu_B = e\hbar/2m_e c$ is the Bohr-Pauli magneton.

In the absence of the scalar and vector potentials, Eq. (22) is used to obtain the relativistic free particle Dirac equation (Gerritsma *et al.*, 2010; Thaller, 1992)

$$i\hbar \frac{\partial \psi}{\partial t} = (c\boldsymbol{\alpha} \cdot \hat{\mathbf{p}} + \beta mc^2) \psi. \quad (24)$$

A general Dirac spinor can be decomposed into parts with positive and negative energies $\mathcal{E} = \pm\sqrt{p^2c^2 + m^2c^4}$. For a free electron, the relativistic Dirac equation predict the Zitterbewegung [arising from an interference effect between the positive and negative energy parts of the spinor, and it does not appear for spinors which consist entirely of positive (or negative-energy) part; it is only present when positive and negative energy parts have significant overlap in position and momentum space] to have an amplitude of the order of the Compton wavelength $\lambda_{\hbar} = \hbar/m_e c = 10^{-10}$ cm. The existence of the Zitterbewegung effect, which has not yet been experimentally accessible, in relativistic quantum mechanics and in quantum field theory is still under debate. Quantum simulation of the one-dimensional Dirac equation has been carried out by Gerritsma *et al.* (2010) to understand the behavior (especially the Zitterbewegung effect) of a free-relativistic electron.

The non-relativistic Pauli equation (Berestetskii *et al.*, 1999) in the presence of the electromagnetic fields describes the dynamics of a single quantum particle. The Pauli equation reads (Tsintsadze and Tsintsadze, 2009)

$$i\hbar \frac{\partial \psi_{\alpha}}{\partial t} = H_{\alpha} \psi_{\alpha}, \quad (25)$$

where

$$H_{\alpha} = -\frac{\hbar^2}{2m_{\alpha}} \nabla^2 + V(\mathbf{A}, \phi), \quad (26)$$

with

$$V(\mathbf{A}, \phi) = \frac{ie\hbar}{2m_{\alpha}c} (\mathbf{A} \cdot \nabla + \nabla \mathbf{A}) + \frac{e^2 \mathbf{A}^2}{2m_{\alpha}c^2} + q_{\alpha} \phi - \mu_{\alpha} \cdot \mathbf{B}. \quad (27)$$

Here $\psi_{\alpha}(\mathbf{r}, t, \sigma)$ is the wave function of the single quantum particle species α with the spin $\mathbf{s} = (1/2)\boldsymbol{\sigma}$ ($|\sigma| = \pm 1$), and $q_{\alpha} = -e$ ($+e$) for electrons (positrons). The last term in (23) is the potential energy of the magnetic dipole in the external magnetic field, the magnetic moment of which is $\mu_{\alpha} = (q_{\alpha}\hbar/2m_{\alpha}c)\boldsymbol{\sigma} \equiv \mu_B\boldsymbol{\sigma}$, where $\boldsymbol{\sigma}$ is the operator of a single quantum particle (Landau and Lifshitz, 1998a).

By using the Madelung representation (Madelung, 1926) for the complex wave function ψ_{α} , viz.

$$\psi_{\alpha}(\mathbf{r}, t, \sigma) = \Psi_{\alpha}(\mathbf{r}, t, \sigma) \exp(iS_{\alpha}/\hbar), \quad (28)$$

where $\Psi_{\alpha}(\mathbf{r}, t, \sigma)$ and $S_{\alpha}(\mathbf{r}, t, \sigma)$ are real, in the Pauli equation (22), we obtain the quantum Madelung fluid equations (Tsintsadze and Tsintsadze, 2009)

$$\frac{\partial n_{\alpha}}{\partial t} + \nabla \cdot (n_{\alpha} \mathbf{p}_{\alpha}/m_{\alpha}) = 0, \quad (29)$$

and

$$\frac{d\mathbf{p}_{\alpha}}{dt} = q_{\alpha} \left(\mathbf{E} + \frac{\mathbf{u}_{\alpha} \times \mathbf{B}}{c} \right) + \mathbf{F}_Q + \mathbf{F}_s, \quad (30)$$

where we have denoted

$$\mathbf{F}_Q = \frac{\hbar^2}{2m_{\alpha}} \nabla \cdot \left(\frac{\nabla^2 n_{\alpha}}{\sqrt{n_{\alpha}}} \right), \quad (31)$$

and

$$\mathbf{F}_s = \mu_B \nabla (\boldsymbol{\sigma} \cdot \mathbf{B}). \quad (32)$$

Here $n_{\alpha} = |\Psi_{\alpha}|^2$ is the probability density of finding a single quantum particle with a spin \mathbf{s} at some point in space, $\mathbf{p}_{\alpha} = \nabla S_{\alpha} - q_{\alpha} \mathbf{A}/c$ is the momentum operator of a quantum particle, $d/dt = (\partial/\partial t) + \mathbf{u}_{\alpha} \cdot \nabla$, \mathbf{u}_{α} is the velocity of a quantum particle, and $\mathbf{E} = -\nabla\phi - c^{-1}\partial\mathbf{A}/\partial t$ and $\mathbf{B} = \nabla \times \mathbf{A}$. We note that the third (the quantum Madelung Force \mathbf{F}_Q) term in the right-hand side of (30) describes the diffraction pattern of a single quantum particle (electron/positron).

The spin force \mathbf{F}_s in matter with non-degenerate quantum particles can also be written as (Brodin and Marklund, 2007a,b,c; Brodin *et al.*, 2008; Marklund and Brodin, 2007)

$$\mathbf{F}_s = \mu_B \tanh \left(\frac{\mu_B B}{k_B T_{\alpha}} \right) \nabla B, \quad (33)$$

where $B = |\mathbf{B}|$ and $\tanh(\xi) = B_{1/2}(\xi)$, with the Brillouin function with argument "1/2" describing particles of spin 1/2. The Langevin parameter $\tanh(\xi)$ accounts for the macroscopic magnetization of the electrons owing to the electron thermal motion and electron-electron collisions.

In the absence of the electromagnetic fields and the quantum particle spin effect, we obtain from (29) and (30) the frequency of quantum oscillations of a free electron

$$\omega_q = \frac{\hbar k^2}{2m_e}, \quad (34)$$

where k is the wave number.

C. The Schrödinger and Wigner-Poisson Equations

The quantum N -body problem is governed by the Schrödinger equation for the N -particle wave function $\psi(q_1, q_2, \dots, q_N)$, where $q_j = (\mathbf{r}_j, s_j)$ is the coordinate (space, spin) of the particle species j , each particle associated with energy \mathcal{E}_j . A drastic simplification occurs if one neglects the correlation between the particles for every order in Γ_Q and describes the full wave function as the product of the single particle wave functions. For identical quantum particles, the N -particle wave function is given by the Slater determinant (Bransden, 2000)

$$\psi(q_1, q_2, \dots, q_N) = \frac{1}{\sqrt{N!}} \times \begin{vmatrix} \psi_1(q_1, t) & \psi_2(q_1) & \cdots & \psi_N(q_1) \\ \psi_1(q_2, t) & \psi_2(q_2) & \cdots & \psi_N(q_2) \\ \vdots & \vdots & \ddots & \vdots \\ \psi_1(q_N) & \psi_2(q_N) & \cdots & \psi_N(q_N) \end{vmatrix}, \quad (35)$$

which is anti-symmetric under odd numbers of permutations. Hence, ψ vanishes if two rows are identical, which is an expression of Pauli's exclusion principle that two identical quantum particles cannot occupy the same state. Example ($N = 2$): $\psi(q_1, q_2) = \frac{1}{\sqrt{2}}[\psi_1(q_1)\psi_2(q_2) - \psi_1(q_2)\psi_2(q_1)]$ so that $\psi(q_2, q_1) = -\psi(q_1, q_2)$ and $\psi(q_1, q_1) = 0$. Due to Pauli's exclusion principle, two degenerate electrons are not allowed to occupy the same quantum state, and in the zero Fermi-temperature limit when all energy states up to the Fermi energy level are occupied by degenerate electrons, there is still a quantum-statistical pressure determined by the Fermi pressure.

The dynamics of an electron interacting with both background electrons and positive ions is governed by the nonlinear equation

$$i\hbar \frac{\partial \psi_i}{\partial t} = H_0 \psi_i, \quad (36)$$

where we have denoted the Hamiltonian $H_0 = -(\hbar^2/2m_e)\nabla^2 + U(|\psi_i|^2) - e\phi$ with the potential (Dvornikov, 2009)

$$U(|\psi_i|^2) = e^2 \int d^3 \mathbf{r}' \frac{1}{|\mathbf{r} - \mathbf{r}'|} [|\psi_i(\mathbf{r}', t)|^2 - n_i(\mathbf{r}', t)], \quad (37)$$

representing the interaction of an electron with background plasma particles which include electrons and ions with the number density $n_i(\mathbf{r}, t)$. In (36) the wave function $\psi(\mathbf{r}, t)$ is normalized to the electron number density such that $n_e(\mathbf{r}, t) = |\psi(\mathbf{r}, t)|^2$. The electrostatic potential is determined from Poisson's equation

$$\nabla^2 \phi = 4\pi e \left(\sum_{i=1}^N \langle |\psi_i|^2 \rangle - n_i \right), \quad (38)$$

where $i = 1, \dots, N$ represent the numbers the electrons as described by pure states, with ψ_i being the wave function for each such state. The angular bracket denotes the Klimontovich statistical average. The statistical averaging becomes important when the wave function contains stochastically varying phase (Anderson *et al.*, 2002).

However, in quantum plasmas with an ensemble of electrons, it is more appropriate to use the quantum statistical theory involving the Wigner-Moyal quasi-particle distribution function (Moyal, 1949; Wigner, 1932)

$$f_w(\mathbf{r}, \mathbf{v}) = \left(\frac{m_e}{2\pi\hbar} \right)^3 \int d\mathbf{R} \exp(i\varphi) \psi^*(\mathbf{r} + \mathbf{R}/2) \psi(\mathbf{r} - \mathbf{R}/2), \quad (39)$$

where $\varphi = m_e \mathbf{v} \cdot \mathbf{R}/\hbar$.

The non-relativistic quantum kinetic equation in the presence of the electrostatic potential is (Haas *et al.*, 2010; Shukla and Eliasson, 2010)

$$\frac{\partial f_w}{\partial t} + \mathbf{v} \cdot \nabla f_w + \int d\mathbf{v}' K(\mathbf{r}, \mathbf{v}' - \mathbf{v}) f_w(\mathbf{v}', \mathbf{r}), \quad (40)$$

for the Wigner-Moyal function. We have denoted

$$K(\mathbf{r}, \mathbf{v}' - \mathbf{v}) = \frac{ie}{\hbar} \left(\frac{m_e}{2\pi\hbar} \right)^3 \int d\mathbf{R} \exp(i\varphi) F(\phi), \quad (41)$$

where $F(\phi) = \phi(\mathbf{r} + \mathbf{R}/2) - \phi(\mathbf{r} - \mathbf{R}/2)$, and the scalar potential ϕ is determined from Poisson's equation

$$\nabla^2 \phi = 4\pi e \left(\int d\mathbf{v} f_w(\mathbf{r}, \mathbf{v}) - n_i \right). \quad (42)$$

The Wigner-Moyal-Poisson equations to a leading order (in the weak quantum coupling parameter Γ_Q) can be written as

$$\begin{aligned} \frac{\partial f_w}{\partial t} + \mathbf{v} \cdot \nabla f_w &= -\frac{iem_e^3}{(2\pi)^3 \hbar^4} \iint e^{im_e(\mathbf{v}-\mathbf{v}') \cdot \mathbf{R}/\hbar} \\ &\times \left[\phi\left(\mathbf{x} + \frac{\mathbf{R}}{2}, t\right) - \phi\left(\mathbf{x} - \frac{\mathbf{R}}{2}, t\right) \right] \\ &\times f_w(\mathbf{x}, \mathbf{v}', t) d^3 R d^3 v' \end{aligned} \quad (43)$$

and

$$\nabla^2 \phi = 4\pi e \left(\int f_w d^3 v - n_0 \right), \quad (44)$$

where non-degenerate ions are assumed immobile.

D. The QHD Equations

The non-relativistic QHD equations (Gardner and Ringhofer, 1996; Manfredi, 2005; Manfredi and Haas, 2001) have been developed in condensed matter physics (Gardner and Ringhofer, 1996) and in plasma physics. The non-relativistic QHD equations are composed of the electron continuity equation

$$\frac{\partial n_e}{\partial t} + \nabla \cdot (n_e \mathbf{u}_e) = 0, \quad (45)$$

the electron momentum equation

$$m_e \left(\frac{\partial \mathbf{u}_e}{\partial t} + \mathbf{u}_e \cdot \nabla \mathbf{u}_e \right) = e \nabla \phi - \frac{1}{n_e} \nabla P_e + \mathbf{F}_Q, \quad (46)$$

and Poisson's equation.

In quantum plasmas with non-relativistic degenerate electrons, one often models the quantum statistical pressure as (Manfredi and Haas, 2001)

$$P_e = \frac{m_e V_{Fe}^2 n_0}{3} \left(\frac{n_e}{n_0} \right)^{(D+2)/D}, \quad (47)$$

where D is the number of degrees of freedom in the system, and $V_{Fe} = (\hbar/m_e)(3\pi^2 n_e)^{1/3}$ is the Fermi electron thermal speed.

E. The NLS-Poisson Equations

For investigating nonlinear properties of dense quantum plasmas, it is appropriate to work with a nonlinear Schrödinger equation. Hence, by introducing the wave function

$$\psi(\mathbf{r}, t) = \sqrt{n_e(\mathbf{r}, t)} \exp\left(i \frac{S_e(\mathbf{r}, t)}{\hbar}\right), \quad (48)$$

where S_e is defined according to $m_e \mathbf{u}_e = \nabla S_e$ and $n_e = |\psi|^2$, it can be readily shown that (46) can be cast as a NLS equation (Manfredi, 2005; Manfredi and Haas, 2001; Shukla, 2006; Shukla and Eliasson, 2006)

$$i\hbar \frac{\partial \psi}{\partial t} + \frac{\hbar^2}{2m_e} \nabla^2 \psi + e\phi \psi - \frac{m_e V_{Fe}^2}{2n_0^2} |\psi|^{4/D} \psi = 0, \quad (49)$$

where the electrostatic field ϕ is determined from Poisson's equation

$$\nabla^2 \phi = 4\pi e(|\psi|^2 - n_0). \quad (50)$$

We note that the NLS equation (49) includes nonlinearities associated with the nonlinear quantum statistical pressure and the nonlinear coupling between the electron wave function and the electrostatic potential.

IV. LINEAR WAVES IN QUANTUM PLASMAS

Linearization of the NLS-Poisson Equations (49) and (50) about the equilibrium state and combining the resultant equations, we obtain the frequency ω of the EPOs (Bohm, 1953; Bohm and Pines, 1953; Klimontovich and Silin, 1952a,b)

$$\omega = \left(\omega_{pe}^2 + \frac{3}{5} k^2 V_{Fe}^2 + \frac{\hbar^2 k^4}{4m_e^2} \right)^{1/2}, \quad (51)$$

where \mathbf{k} is the wave vector and $\omega_{pe} = (4\pi n_0 e^2 / m_e)^{1/2}$ is the electron plasma frequency.

One can identify two distinct dispersive effects from (51): One long wavelength regime with $V_{Fe} \gg \hbar k / 2m_e$, and the other short wavelength regime with $V_{Fe} \leq \hbar k / 2m_e$. These two regimes are separated by the critical wavenumber

$$k_{crit} = \frac{2\pi}{\lambda_{crit}} \approx \frac{\pi \hbar}{m_e V_{Fe}} \sim n_e^{-1/3}. \quad (52)$$

It should be mentioned here that the quantum dispersion effects associated with the EPOs have recently been observed in compressed plasmas (Glenzer *et al.*, 2007; Neumayer *et al.*, 2010). In the compressed plasma experiments, powerful x-ray sources are employed for accessing narrow bandwidth electron plasma wave spectral lines via collective Thomson scattering in which powerful light scatters off electron-density fluctuations.

Furthermore, letting $\psi_i(\mathbf{r}, t) = \psi_0 + \psi_{1k} \exp(-i\omega t)$ in (36) without the ϕ term, where $|\psi_0|^2 = n_0$ and $\psi_{1k} \propto (1/r) \sin(kr)$, we obtain the dispersion relation (Dvornikov, 2009) for spherically symmetric quantum oscillations in an electron plasma. We have

$$k_{\pm}^2 = \frac{m_e \omega}{\hbar} \left[1 \pm \left(1 - 4 \frac{\omega_{pe}^2}{\omega^2} \right)^{1/2} \right], \quad (53)$$

which exhibits two branches for the functions $y_{\pm} = k_{\pm} \sqrt{\hbar / 2\omega_{pe} m_e}$ against $\Omega = \omega / \omega_{pe}$. The upper (represented by +) and lower (represented by -) branches are related with the high- and low-energy solutions.

In the remote past many authors derived the dielectric constant for electrostatic waves (Bohm, 1953; Bohm and Pines, 1953; Klimontovich and Silin, 1952a,b; Lifshitz and Pitaevskii, 1981) and the refractive index for the electromagnetic wave (Burt and Wahlquist, 1962) by using the quantum kinetic theory based on the Wigner equation and the Poisson-Maxwell equations in quantum plasmas. In the following, we present the well known results for electrostatic (Bohm, 1953; Bohm and Pines, 1953; Klimontovich and Silin, 1952a,b) and electromagnetic (Burt and Wahlquist, 1962) waves in an unmagnetized quantum plasma.

The dielectric constant for electrostatic waves in a plasma with completely degenerate electrons reads (Lif-

shitz and Pitaevskii, 1981)

$$D_e(\omega, \mathbf{k}) = 1 + \frac{3\omega_{pe}^2}{2k^2V_{Fe}^2} [1 - g(\omega_+) - g(\omega_-)], \quad (54)$$

where $\omega_{\pm} = \omega \pm \hbar k^2/2m_e$, and in the zero Fermi temperature limit, we have

$$g(\omega) = \frac{m_e(\omega^2 - k^2V_{Fe}^2)}{2\hbar k^3V_{Fe}} \log\left(\frac{\omega + kV_{Fe}}{\omega - kV_{Fe}}\right). \quad (55)$$

Assuming that the phase velocity (ω/k) of the wave is much larger than V_{Fe} , we obtain by setting $D_e(\omega, \mathbf{k}) = 0$ the frequency of the EPOs, given by (51). On the other hand, in the quasi-classical limit, viz. $\hbar k \ll p_{Fe} = \hbar(3\pi^2n_e)^{1/3}$, we have (Lifshitz and Pitaevskii, 1981) from Eq. (54)

$$D_e(\omega, \mathbf{k}) = 1 + \frac{3\omega_{pe}^2}{k^2V_{Fe}^2} \left(1 - \frac{\omega}{kV_{Fe}} \log\left|\frac{\omega + kV_{TF}}{\omega - kV_{TF}}\right|\right), \quad (56)$$

which in the short wavelength limit, viz. $kV_{Fe} \gg \omega_{pe}$, yields the well known zero sound wave (Klimontovich and Silin, 1952a,b, 1961)

$$\omega = kV_{Fe} [1 + 2 \exp(-2k^2\lambda_{TF}^2 - 2)], \quad (57)$$

where $\lambda_{TF} = V_{Fe}/\sqrt{3}\omega_{pe}$ is the Thomas-Fermi screening length.

Furthermore, when $\omega = 0$, the expression (56) as a function of k has a Kohn singularity at $\hbar k = 2p_{Fe} \equiv$ the diameter of the Fermi sphere. Here we have

$$D_e(0, \mathbf{k}) = 1 + \frac{e^2}{2\pi\hbar E_F} [1 - \xi \log(1/|\xi|)], \quad (58)$$

where $\xi = (\hbar k - 2p_{Fe})/2p_{Fe}$ and $|\xi| \ll 1$. In quantum plasmas, with $D(0, \mathbf{k})$ given by (58), the potential distribution $\varphi(r)$ around a stationary test charge q_t is

$$\varphi(r) = \frac{4\pi q_t}{(2\pi)^3} \int \frac{\exp(i\mathbf{k} \cdot \mathbf{r}) d^3k}{k^2 D_e(0, \mathbf{k})}, \quad (59)$$

which gives (Else *et al.*, 2010)

$$\varphi(r) \approx q_t \frac{36\lambda_{TF}^2 \eta^4}{(2 + 3\eta^2)^2} \frac{\cos(2k_F r)}{r^3}, \quad (60)$$

where $\eta = \hbar\omega_{pe}/4k_B T_{Fe}$ and $k_F = p_{Fe}/\hbar$. We note (60), which is proportional to $r^{-3} \cos(2k_F r)$ considerably differs from the Debye-Hückel shielding potential that is proportional to $r^{-1} \exp(-r/\lambda_{De})$ in a classical plasma with the Boltzmann-Maxwell electron distribution function. Here λ_{De} is the electron Debye radius. We further note that the shielding of a moving test charge in an unmagnetized quantum plasma has been investigated by Else *et al.* (2010) both analytically and numerically.

We now focus our attention on the effects of the dynamics of non-degenerate ions in an unmagnetized quantum plasma. The ion dynamics is governed by the continuity and momentum equations

$$\frac{\partial n_i}{\partial t} + \nabla \cdot (n_i \mathbf{u}_i) = 0, \quad (61)$$

and

$$\left(\frac{\partial}{\partial t} + \mathbf{u}_i \cdot \nabla\right) \mathbf{u}_i = -\frac{e}{m_i} \nabla \phi, \quad (62)$$

where n_i is the ion number density, \mathbf{u}_i the ion fluid velocity, and m_i the ion mass. The ions are coupled with the electrons by the space charge electric field $\mathbf{E} = -\nabla \phi$, where

$$\nabla^2 \phi = 4\pi e(n_e - Z_i n_i). \quad (63)$$

For the low-phase velocity (in comparison with the Fermi electron thermal speed) electrostatic waves, one can neglect the inertia of electrons and obtain

$$n_e \nabla \phi - \frac{(3\pi^2)^{2/3}}{5} \frac{\hbar^2}{m_e} \nabla n_e^{5/3} + \frac{\hbar^2 n_e}{2m_e} \nabla \left(\frac{\nabla^2 n_e}{\sqrt{n_e}}\right) = 0, \quad (64)$$

for a quantum plasma with weakly relativistic degenerate electrons, while for a quantum plasma with ultra-relativistic degenerate electrons, we have

$$n_e \nabla \phi - \frac{(3\pi^2)^{1/3}}{4} \hbar c \nabla n_e^{4/3} = 0. \quad (65)$$

Due to the ion motion, one would have new dielectric constants for the low-frequency electrostatic waves (Eliasson and Shukla, 2008a; Mushtaq and Melrose, 2009; Pines, 1963; Pines and Nozieres, 1989; Shukla and Eliasson, 2008b). In a quantum plasma with non-relativistic degenerate electrons with $\omega^2 \ll k^2 V_{Fe}^2 + \hbar^2 k^4/4m_e^2$, we have

$$D_i(\omega, \mathbf{k}) = 1 + \frac{\omega_{pe}^2}{k^2 V_{Fe}^2 + \hbar^2 k^4/4m_e^2} - \frac{\omega_{pi}^2}{\omega^2}, \quad (66)$$

where $\omega_{pi} = (4\pi n_0 e^2/m_i)^{1/2}$ is the ion plasma frequency. On the other hand, in a very dense plasma with the ultra-relativistic degenerate electrons, we have

$$D_i(\omega, \mathbf{k}) = 1 + \frac{\omega_{pe}^2}{k^2 C_h^2} - \frac{\omega_{pi}^2}{\omega^2}, \quad (67)$$

where we have denoted $C_h^2 = (4/3)c^2 \lambda_C n_0^{1/3}$, and $\lambda_C = \hbar/m_e c$ is the Compton length.

By setting $D_i(\omega, \mathbf{k}) = 0$, we obtain the frequencies of the ion waves in our quantum plasmas. We have (Stenflo and Shukla, 2009)

$$\omega = \frac{\omega_{pi} k \lambda_{T\hbar}}{(1 + k^2 \lambda_{T\hbar}^2)^{1/2}}, \quad (68)$$

for the no-relativistic degenerate electrons, and (Shukla, 2010)

$$\omega = \frac{\omega_{pi} k \lambda_{\hbar}}{(1 + k^2 \lambda_{\hbar}^2)^{1/2}}, \quad (69)$$

for the ultra-relativistic degenerate electrons. Here we have denoted $\lambda_{T\hbar} = [(V_{TF}^2/\omega_{pe}^2) + \hbar^2 k^4/4m_e^2 \omega_{pe}^2]^{1/2}$, and $\lambda_{\hbar} = C_h/\omega_{pe}$.

Melrose and Mushtaq (2009) and Mushtaq and Melrose (2009) have presented Landau damping rates for both electron and ion plasma waves in an unmagnetized dense quantum plasma. The imaginary parts of the dielectric constants can be used to calculate the structural form factor in plasmas with degenerate electrons (Ichimaru, 1982).

Shukla and Eliasson (2008b) used the dielectric constant (66) without the quantum statistical pressure term (viz. the V_{Fe}^2 -term) to investigate the screening and wake potentials around a test charge in an electron-ion quantum plasma. They found a new screening potential (Shukla and Eliasson, 2008b)

$$\phi_{se} = \frac{qt}{r} \exp(-k_q r) \cos(k_q r), \quad (70)$$

and the wake potential

$$\phi_w = -\frac{qt}{|z - u_0 t|} \cos\left[\frac{\omega_{pi}}{u_0}(z - u_0 t)\right], \quad (71)$$

where $k_q = \sqrt{2}/\sqrt{\hbar/m_e \omega_{pe}}$ is the quantum wave number, and $r = [x^2 + y^2 + (z - u_0 t)^2]^{1/2}$ the distance from the test charge moving with the speed u_0 along the z axis in a Cartesian co-ordinate system. The wake potential behind a test charge arises due to collective interactions between a test charge and the ion oscillation with the frequency $\omega_k \approx \omega_{pi} k_{\perp}^2 / (k_{\perp}^2 + k_q^2)^{1/2}$, with $k_z \ll k_q$, $k_{\perp} = (k_x^2 + k_y^2)^{1/2}$. We note that the Shukla-Eliasson (SE) exponential cosine-screened Coulomb potential ϕ_{se} has a minimum of $\phi_{se} \approx -0.02qt k_q$ at $r \approx 3k_q^{-1}$, similar to the Lennart-Jones potential for atoms. The SE screening potential ϕ_{se} is independent of the test charge speed u_0 . Recently, several authors (Ghoshal and Ho, 2009a,b; Xia *et al.*, 2010) have used the Shukla-Eliasson potential to study doubly excited resonance states of Helium and hydrogen atoms embedded in quantum plasmas (Ghoshal and Ho, 2009a,b), as well as lattice waves in two-dimensional hexagonal quantum plasma crystals (Xia *et al.*, 2010).

Furthermore, by using D_i from (67), one can deduce the potential distribution around a moving test charge in a relativistically dense plasma as

$$\phi(r, z) = \frac{qt}{r} \exp\left(-\frac{r}{\Lambda_C}\right) + \frac{qt}{|z - u_0 t|} \cos[(z - u_0 t)/L_c], \quad (72)$$

where $\Lambda_C = C_{\hbar}/\omega_{pe}$ and $L_c = \lambda_c (M^2 - 1)^{1/2} > 0$, with $M = u_0/C_{\hbar}$.

Finally, we turn our attention to the high-frequency electromagnetic (HF-EM) waves in an unmagnetized quantum plasma. Noting that the HF-EM waves in the latter do not give rise to any density perturbations, we have the EM wave frequency

$$\omega = (k^2 c^2 + \omega_{pe}^2)^{1/2}. \quad (73)$$

However, consideration of the electron spin current and electron exchange potential contributions in a quantum

plasma gives rise to additional contributions to the refractive index. We have (Burt and Wahlquist, 1962)

$$\frac{k^2 c^2}{\omega^2} = N \approx 1 - \frac{\omega_{pe}^2}{\omega^2} - \frac{\omega_{pe}^2 \hbar^2 k^2}{m_e^2 \omega^4} \left(\frac{1}{5} K_F^2 + \frac{1}{4} k^2 \right), \quad (74)$$

which includes the electron spin correction, and is valid at zero temperature. Here $\hbar K_F = (2m_e E_{Fe})^{1/2}$ is the momentum of degenerate electrons at the top of the Fermi-Dirac distribution, $(1/5)K_F^2$ is related to the leading quantum term from the ordinary transverse current, and the $k^2/4$ term arises from the electron spin interactions. On the other hand, the electromagnetic wave dispersion relation, which accounts for the electron exchange potential and discards the spin correction, reads (Burt and Wahlquist, 1962)

$$\frac{k^2 c^2}{\omega^2} = N \approx 1 - \frac{\omega_{pe}^2}{\omega^2} - \frac{\omega_{pe}^2 \hbar^2 k^2 K_F^2}{5m_e^2 \omega^4} + \frac{3\omega_{pe}^2 k^2}{40\omega^4 K_F^2}. \quad (75)$$

V. QUANTUM DARK SOLITONS AND VORTICES

Let us now discuss the nonlinear properties and dynamics of one-dimensional quantum dark solitons (characterized by the local electron density depletion associated with a positive potential) and two-dimensional azimuthally symmetric electron vortices in dense quantum plasmas (Shukla and Eliasson, 2006).

We shall use the NLS-Poisson equations (Shukla, 2006; Shukla and Eliasson, 2006)

$$i \frac{\partial \Psi}{\partial t} + \mathcal{A} \nabla^2 \Psi + \varphi \Psi - |\Psi|^{4/D} \Psi = 0, \quad (76)$$

and

$$\nabla^2 \varphi = |\Psi|^2 - 1, \quad (77)$$

where the time and space variables are in units of $\hbar/k_B T_{Fe}$ and the Fermi electron Debye radius λ_D , respectively. Furthermore, we have denoted $\Psi = \psi/\sqrt{n_0}$, $\varphi = e\phi/k_B T_{Fe}$, and $\mathcal{A} = 2\pi n_0^{1/3} e^2/k_B T_{Fe}$. The system (76) and (77) is supplemented by

$$\frac{\partial \mathbf{E}_{\varphi}}{\partial t} = i\mathcal{A} (\Psi \nabla \Psi^* - \Psi^* \nabla \Psi), \quad (78)$$

where we have denoted $\mathbf{E}_{\varphi} = -\nabla \varphi$. The system (76)–(78) has the following conserved integrals (Shaikh and Shukla, 2007; Shukla and Eliasson, 2006): the number of electrons

$$N = \int |\Psi|^2 d^3x, \quad (79)$$

the electron momentum

$$\mathbf{P} = -i \int \Psi^* \nabla \Psi d^3x, \quad (80)$$

the electron angular momentum

$$\mathbf{L} = -i \int \Psi^* \mathbf{r} \times \nabla \Psi d^3x, \quad (81)$$

and the total energy

$$\mathcal{E} = \int \left[-\mathcal{A} \Psi^* \nabla^2 \Psi + \frac{|\nabla \varphi|^2}{2} + \frac{D}{(2+D)} |\Psi|^{(2+4/D)} \right] d^3x. \quad (82)$$

A. Quantum Electron Holes

For quasi-stationary, one-dimensional structures moving with a constant speed v_0 , one can find localized, solitary wave solutions by the ansatz $\Psi = W(\xi) \exp(iK_s x - i\Omega_s t)$, where W is a complex-valued function of the argument $\xi = x - v_0 t$, and K_s and Ω_s are a constant wavenumber and frequency shift, respectively. By the choice $K_s = v_0/2\mathcal{A}$, the coupled system of equations can be written as

$$\frac{d^2 W}{d\xi^2} + \lambda W + \frac{\varphi W}{\mathcal{A}} - \frac{|W|^4 W}{\mathcal{A}} = 0, \quad (83)$$

and

$$\frac{d^2 \varphi}{d\xi^2} = |W|^2 - 1, \quad (84)$$

where $\lambda = (\Omega_s/\mathcal{A}) - v_0^2/4\mathcal{A}^2$ is an eigenvalue of the system. From the boundary conditions $|W| = 1$ and $\varphi = 0$ at $|\xi| = \infty$, we determine $\lambda = 1/\mathcal{A}$ and $\Omega_s = 1 + v_0^2/4\mathcal{A}$. The system of Eqs. (83) and (84) admits a first integral in the form

$$\begin{aligned} H_h &= \mathcal{A} \left| \frac{dW}{d\xi} \right|^2 - \frac{1}{2} \left(\frac{d\varphi}{d\xi} \right)^2 + |W|^2 \\ &- \frac{|W|^6}{3} + \varphi |W|^2 - \varphi - \frac{2}{3} = 0, \end{aligned} \quad (85)$$

where the boundary conditions $|W| = 1$ and $\varphi = 0$ at $|\xi| = \infty$ have been employed.

Figure 2 shows profiles of $|W|^2$ and φ obtained numerically from (83) and (84) for a few values of \mathcal{A} , where W was set to -1 on the left boundary and to $+1$ on the right boundary, i.e. the phase shift is 180 degrees between the two boundaries. The solutions are in the form of dark solitons, with a localized depletion of the electron density $N_e = |W|^2$, associated with a localized positive potential. Larger values of the quantum coupling parameter \mathcal{A} give rise to larger-amplitude and wider dark solitons. The solitons localized “shoulders” on both sides of the density depletion.

Numerical solutions of the time-dependent system of Eqs. (76) and (77) is displayed in Fig. 3, with initial conditions close (but not equal) to the ones in Fig. 2. Two very clear and long-lived dark solitons are visible, associated with a positive potential of $\varphi \approx 3$, in agreement with the quasi-stationary solution of Fig. 2 for

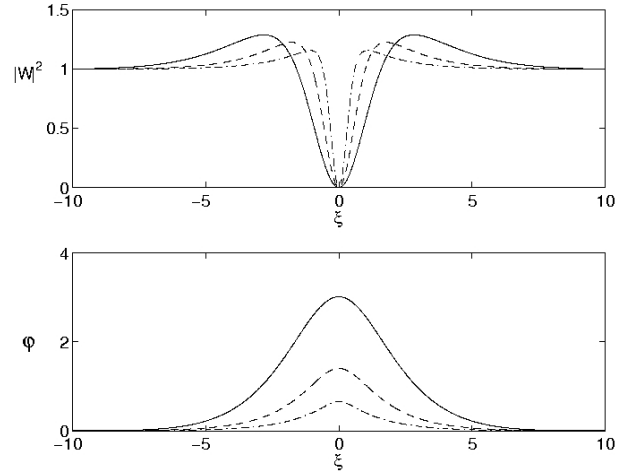


FIG. 2 The electron density $|W|^2$ (the upper panel) and electrostatic potential φ (the lower panel) associated with a dark soliton supported by the system of equations (83) and (85), for $\mathcal{A} = 5$ (solid lines), $\mathcal{A} = 1$ (dashed lines), and $\mathcal{A} = 0.2$ (dash-dotted line). After Shukla and Eliasson (2006).

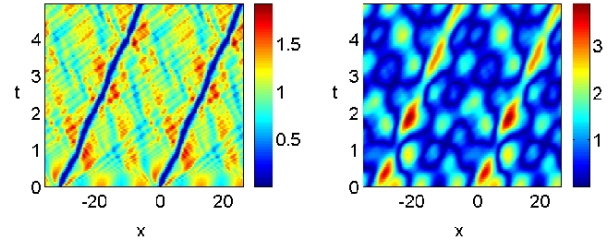


FIG. 3 The time-development of the electron density $|\Psi|^2$ (left-hand panel) and electrostatic potential φ (the right-hand panel), obtained from a simulation of the system of equations (76) and (77). The initial condition is $\Psi = 0.18 + \tanh[20 \sin(x/10)] \exp(iK_s x)$, with $K_s = v_0/2\mathcal{A}$, $\mathcal{A} = 5$ and $v_0 = 5$. After Shukla and Eliasson (2006).

$\mathcal{A} = 5$. In addition there are oscillations and wave turbulence in the time-dependent solution presented in Fig. 3. Hence, the dark solitons seem to be robust structures that can withstand perturbations and turbulence during a considerable time.

B. Quantum Electron Vortices

For two-dimensional ($D = 2$) EPOs in quantum plasmas, one can look for quantum vortex structures of the form $\Psi = \psi(r) \exp(is\theta - i\Omega_v t)$, where r and θ are the polar coordinates defined via $x = r \cos(\theta)$ and $y = r \sin(\theta)$, Ω_v is a constant frequency shift, and $s = 0, \pm 1, \pm 2, \dots$ for different excited states (charge states). With this ansatz, Eqs. (76) and (77) can be written as, respectively,

$$\left[\Omega_v + \mathcal{A} \left(\frac{d^2}{dr^2} + \frac{1}{r} \frac{d}{dr} - \frac{s^2}{r^2} \right) + \varphi - |\psi|^2 \right] \psi = 0, \quad (86)$$

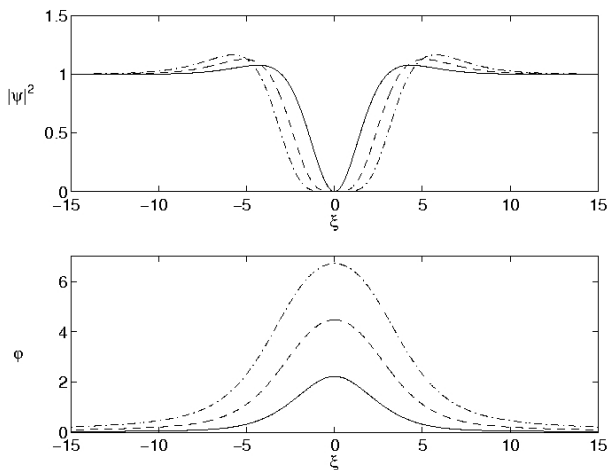


FIG. 4 The electron density $|\Psi|^2$ (upper panel) and electrostatic potential φ (lower panel) associated with a two-dimensional vortex supported by the system (86) and (87), for the charge states $s = 1$ (solid lines), $s = 2$ (dashed lines) and $s = 3$ (dash-dotted lines). We used $\mathcal{A} = 5$ in all cases. After Shukla and Eliasson (2006).

and

$$\left(\frac{d^2}{dr^2} + \frac{1}{r} \frac{d}{dr} \right) \varphi = |\psi|^2 - 1, \quad (87)$$

where the boundary conditions $\psi = 1$ and $\varphi = d\psi/dr = 0$ at $r = \infty$ determine the constant frequency $\Omega_v = 1$. Different signs of the charge state s describe different rotation directions of the quantum vortex. For $s \neq 0$, one must have $\psi = 0$ at $r = 0$, and from symmetry considerations one has $d\varphi/dr = 0$ at $r = 0$. Figure 4 depicts numerical solutions of Eqs. (86) and (87) for different values of s and for $\mathcal{A} = 5$. Here a quantum vortex is characterized by a complete depletion of the electron density at the core of the vortex, and is associated with a positive electrostatic potential.

Figure 5 exhibits time-dependent solutions of Eqs. (76) and (77) in two-space dimensions for singly charged ($s = \pm 1$) vortices, where, in the initial condition, four vortex-like structures were placed at some distance from each other. The initial conditions were such that the vortices are organized in two vortex pairs, with $s_1 = +1$, $s_2 = -1$, $s_3 = -1$, and $s_4 = +1$, seen in the upper panels of Fig. 5. The vortices in the pairs have opposite polarity on the electron fluid rotation, as seen in the upper right panel of Fig. 5. Interestingly, the “partners” in the vortex pairs attract each other and propagate together with a constant velocity, and in the collision and interaction of the vortex pairs (see the second and third pairs of panels in Fig. 5), the vortices keep their identities and change partners, resulting into two new vortex pairs which propagate obliquely to the original propagation direction. On the other hand, as shown in Fig. 6, vortices that are multiply charged ($|s_j| > 1$) are unstable. Here the system of Eqs. (76) and (77) was again solved numerically with

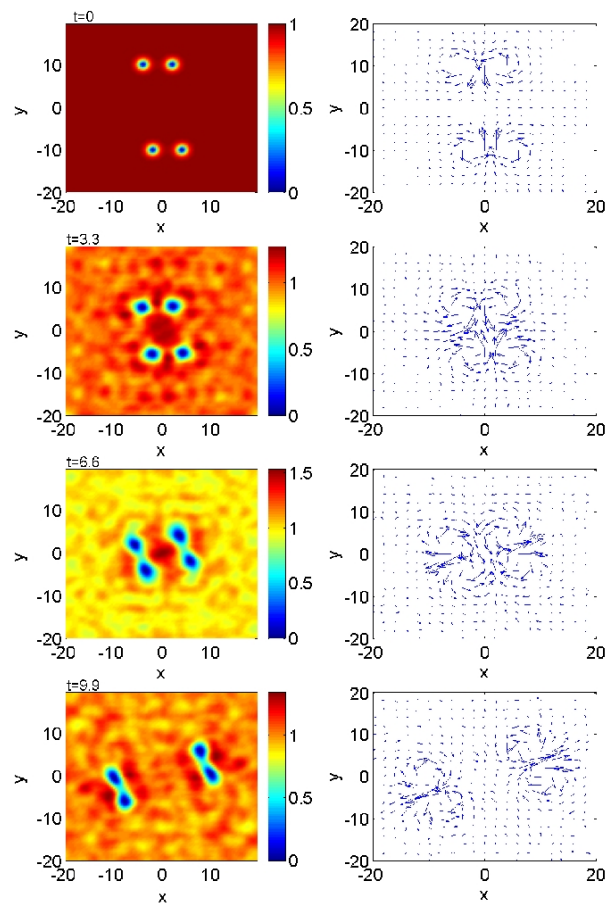


FIG. 5 The electron density $|\Psi|^2$ (left panel) and an arrow plot of the electron current $i(\Psi\nabla\Psi^* - \Psi^*\nabla\Psi)$ (right panel) associated with singly charged ($|s| = 1$) two-dimensional vortices, obtained from a simulation of the time-dependent system of equations (76) and (77), at times $t = 0$, $t = 3.3$, $t = 6.6$ and $t = 9.9$ (upper to lower panels). We used $\mathcal{A} = 5$. The singly charged vortices form pairs and keep their identities. After Shukla and Eliasson (2006).

the same initial condition as the one in Fig. 5, but with doubly charged vortices $s_1 = +2$, $s_2 = -2$, $s_3 = -2$, and $s_4 = +2$. The second row of panels in Fig. 6 reveals that the vortex pairs keep their identities for some time, while a quasi one-dimensional density cavity is formed between the two vortex pairs. At a later stage, the four vortices dissolve into complicated nonlinear structures and wave turbulence. Hence, the nonlinear dynamics is very different between singly and multiply charged solitons, where only singly charged vortices are long-lived and keep their identities.

VI. QUANTUM ELECTRON FLUID TURBULENCE

The statistical properties of turbulence and its associated electron transport at nanoscales in quantum plasmas has been investigated in both 2D and 3D by means of the coupled NLS and Poisson equations (Shaikh and

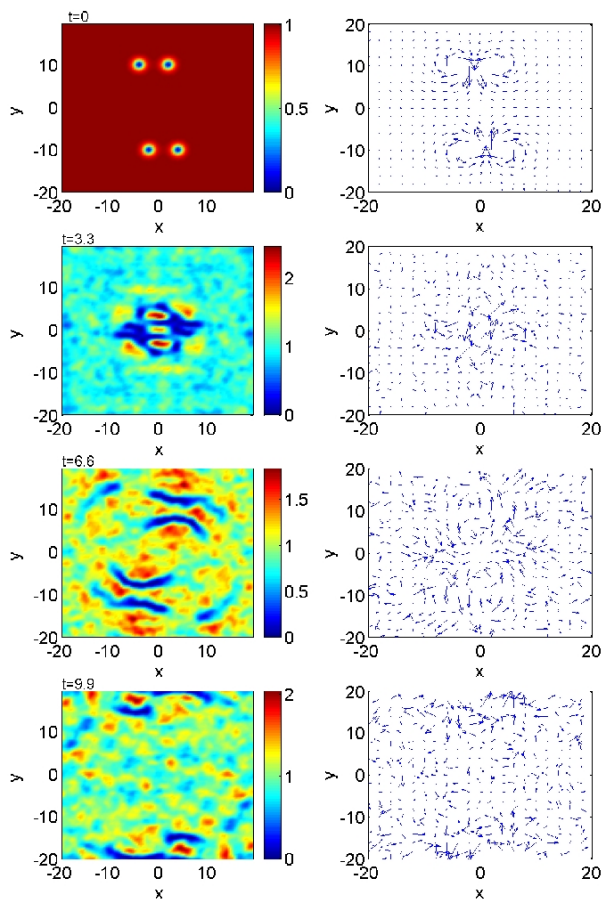


FIG. 6 The electron density $|\Psi|^2$ (left panel) and an arrow plot of the electron current $i(\Psi\nabla\Psi^* - \Psi^*\nabla\Psi)$ (right panel) associated with double charged ($|s| = 2$) two-dimensional vortices, obtained from a simulation of the time-dependent system of Eqs. (76) and (77), at times $t = 0$, $t = 3.3$, $t = 6.6$ and $t = 9.9$ (upper to lower panels). We used $\mathcal{A} = 5$. The doubly charged vortices dissolve into nonlinear structures and wave turbulence. After Shukla and Eliasson (2006).

Shukla, 2007, 2008). It has been found that the nonlinear coupling between the EPOs of different scale sizes gives rise to small-scale electron density structures, while the electrostatic potential cascades towards large-scales. The total energy associated with the quantum electron plasma turbulence, nonetheless, processes a characteristic, *non*-Kolmogorov-like spectrum.

To investigate the quantum electron fluid turbulence in 3D, we use the nonlinear Schrödinger-Poisson equations (Manfredi and Haas, 2001; Shaikh and Shukla, 2008; Shukla, 2006; Shukla and Eliasson, 2006)

$$i\sqrt{2H}\frac{\partial\Psi}{\partial t} + H\nabla^2\Psi + \varphi\Psi - |\Psi|^{4/3}\Psi = 0, \quad (88)$$

and

$$\nabla^2\varphi = |\Psi|^2 - 1, \quad (89)$$

which govern the dynamics of nonlinearly interacting EPOs of different wavelengths. In Eqs. (88) and (89)

the wave function is normalized by $\sqrt{n_0}$, the electrostatic potential by $k_B T_{Fe}/e$, the time t by the electron plasma period ω_{pe}^{-1} , and the space \mathbf{r} by the Fermi electron Debye radius $\lambda_D = V_{Fe}/\omega_{pe}$. We have here introduced the notation $\sqrt{H} = \hbar\omega_{pe}/\sqrt{2}k_B T_{Fe}$.

A. Modeling Methods and Plasma Parameters

The nonlinear wave-wave coupling studies are performed to investigate the multi-scale evolution of a decaying 3D electron fluid turbulence, which is described by Eqs. (88) and (89). All the fluctuations are initialized isotropically (no mean fields are assumed) with random phases and amplitudes in Fourier space, and evolved further by the integration of Eqs. (88) and (89), using a fully de-aliased pseudospectral numerical scheme (Gottlieb and Orzag, 1977) based on the Fourier spectral methods. The spatial discretization in our 3D simulations uses a discrete Fourier representation of turbulent fluctuations. The evolution variables use periodic boundary conditions. The initial isotropic turbulent spectrum was chosen close to k^{-2} , with random phases in all three directions. The choice of such (or even a flatter than -2) spectrum treats the turbulent fluctuations on an equal footing and avoids any influence on the dynamical evolution that may be due to the initial spectral non-symmetry.

We study the properties of 3D fluid turbulence, composed of nonlinearly interacting EPOs, for two specific physical systems. These are the dense plasmas in the next generation laser-based plasma compression (LBPC) schemes (Malkin *et al.*, 2007) as well as in superdense astrophysical objects (Chabrier *et al.*, 2002, 2006; Chabrier, 2009; Harding and Lai, 2006; Lai, 2001) (e.g. white dwarfs). It is expected that in LBPC schemes, the electron number density may reach 10^{27} cm^{-3} and beyond. Hence, we have $\omega_{pe} = 1.76 \times 10^{18} \text{ s}^{-1}$, $T_{Fe} = 1.7 \times 10^{-9} \text{ erg}$, $\hbar\omega_{pe} = 1.7 \times 10^{-9} \text{ erg}$, and $H = 1$. The Fermi electron Debye radius $\lambda_D = 0.1 \text{ \AA}$. On the other hand, in the core of white dwarf stars, we typically have $n_0 \sim 10^{30} \text{ cm}^{-3}$, yielding $\omega_{pe} = 5.64 \times 10^{19} \text{ s}^{-1}$, $T_{Fe} = 1.7 \times 10^{-7} \text{ erg}$, $\hbar\omega_{pe} = 5.64 \times 10^{-8} \text{ erg}$, $H \approx 0.3$, and $\lambda_D = 0.025 \text{ \AA}$. The numerical solutions of Eqs. (88) and (89) for $H = 1$ and $H = 0.025$ (corresponding to $n_0 = 10^{27} \text{ cm}^{-3}$ and $n_0 = 10^{30} \text{ cm}^{-3}$, respectively) are displayed in Figs. 7 and 8, respectively, which are the electron number density and the electrostatic (ES) potential distributions in the (x, y) -plane.

B. Formation of Quantum Structures and Associated Spectra

Figures 7 and 8 reveal that the electron density distribution has a tendency to generate smaller length-scale structures, while the ES potential cascades towards larger scales. The co-existence of the small and larger scale

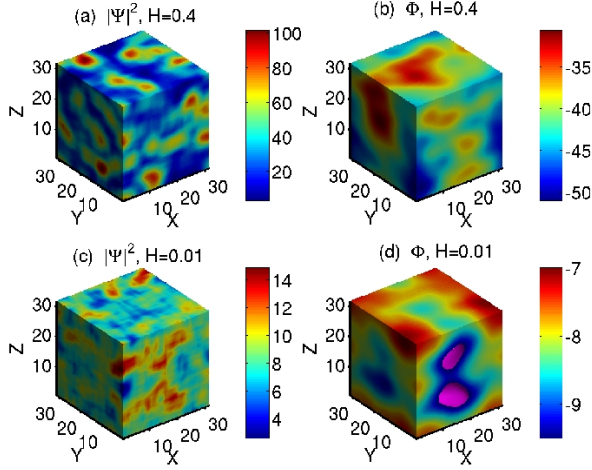


FIG. 7 Small scale fluctuations in the electron density resulted from a steady turbulence simulations of our 3D electron plasma, for $H = 0.4$ (top panels) and $H = 0.01$ (bottom panels). Forward cascades are responsible for the generation of small-scale fluctuations seen in panels (a) and (c). Large scale structures are present in the electrostatic potential, seen in panels (b) and (d), essentially resulting from an inverse cascade. After Shaikh and Shukla (2008).

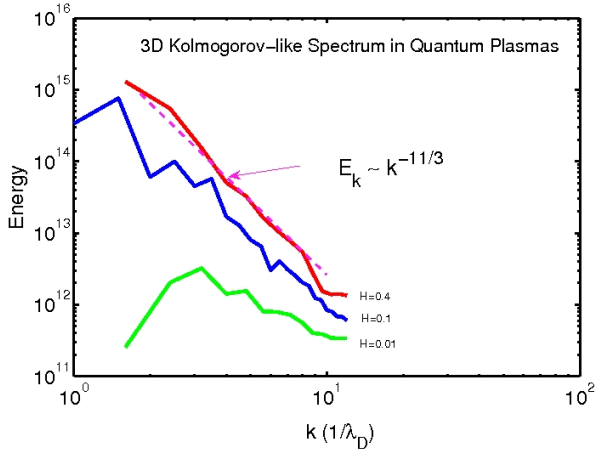


FIG. 8 Power spectrum of 3D EPOs in the forward cascade regime. A Kolmogorov-like spectrum $\sim k^{-11/3}$ is observed for $H = 0.4$. The spectral index changes as a function of H . The numerical resolution is 128^3 . After Shaikh and Shukla (2008).

structures in turbulence is a ubiquitous feature of various 3D turbulence systems. For example, in 3D hydrodynamic turbulence, the incompressible fluid admits two invariants, namely the energy and the mean squared vorticity. The two invariants, under the action of an external forcing, cascade simultaneously in turbulence, thereby leading to a dual cascade phenomena. In these processes, the energy cascades towards longer length-scales, while the fluid vorticity transfers spectral power towards shorter length-scales. Usually, a dual cascade is observed

in a driven turbulence simulation, in which certain modes are excited externally through random turbulent forces in spectral space. The randomly excited Fourier modes transfer the spectral energy by conserving the constants of motion in k -space. On the other hand, in freely decaying turbulence, the energy contained in the large-scale eddies is transferred to the smaller scales, leading to a statistically stationary inertial regime associated with the forward cascades of one of the invariants. Decaying turbulence often leads to the formation of coherent structures as turbulence relaxes, thus making the nonlinear interactions rather inefficient when they are saturated. The power spectrum exhibits an interesting feature in our 3D electron plasma system, unlike the 3D hydrodynamic turbulence (Frisch, 1995; Kolmogorov, 1941; Lesieur, 1990). The spectral slope in the 3D quantum electron fluid turbulence is close to the Iroshnikov-Kraichnan power law (Iroshnikov, 1963; Kraichnan, 1965) $k^{-3/2}$, rather than the usual Kolmogorov power law (Kolmogorov, 1941) $k^{-5/3}$. We further find that this scaling is not universal and is determined critically by the quantum electron tunneling effect. For instance, for a higher value of $H = 1.0$ the spectrum becomes more flat (see Fig 8). Physically, the flatness (or deviation from the $k^{-5/3}$), results from the short wavelength part of the EPOs spectrum which is controlled by the quantum electron tunneling effect associated with the Bohm potential. The peak in the energy spectrum can be attributed to the higher turbulent power residing in the EPO potential, which eventually leads to the generation of larger scale structures, as the total energy encompasses both the electrostatic potential and electron density components. In our dual cascade process, there is a delicate competition between the EPO dispersions caused by the statistical pressure law (giving the $k^2 V_{Fe}^2$ term, which dominates at longer scales) and the quantum Bohm force (giving the $\hbar^2 k^4 / 4m_e^2$ term, which dominates at shorter scales with respect to a source).

We finally estimate the electron diffusion coefficient in the presence of small and large scale turbulent EPOs in our quantum plasma. An effective electron diffusion coefficient caused by the momentum transfer can be calculated from $D_{eff} = \int_0^\infty \langle \mathbf{P}(\mathbf{r}, t) \cdot \mathbf{P}(\mathbf{r}, t+t') \rangle dt'$, where \mathbf{P} is electron momentum and the angular bracket denotes spatial averages and the ensemble averages are normalized to unit mass. The effective electron diffusion coefficient, D_{eff} , essentially relates the diffusion processes associated with random translational motions of the electrons in nonlinear plasmonic fields. We compute D_{eff} in our simulations, to measure the turbulent electron transport that is associated with the turbulent structures that we have reported herein. It is observed that the effective electron diffusion is lower when the field perturbations are Gaussian. On the other hand, the electron diffusion increases rapidly with the eventual formation of longer length-scale structures, as shown in Fig. 9. The electron diffusion due to large scale potential distributions in quantum plasmas dominates substantially, as depicted by the solid-curve in Fig. 9. Furthermore, in the steady-

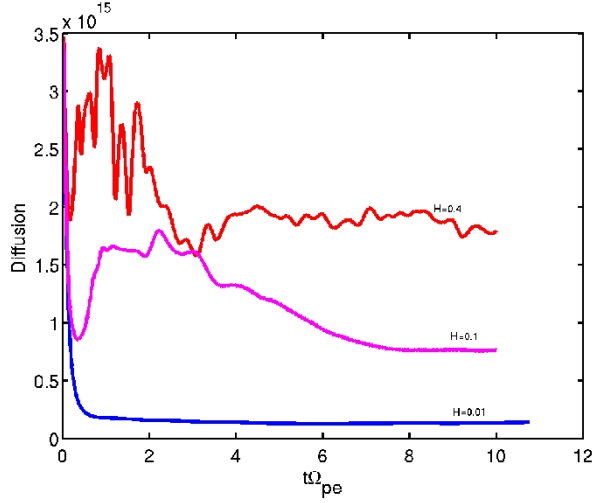


FIG. 9 Time evolution of an effective electron diffusion coefficient associated with the large-scale electrostatic potential and the small-scale electron density, for $H = 0.4$, $H = 0.1$ and $H = 0.01$. Smaller values of H corresponds to a small effective diffusion coefficient, which characterizes the presence of small-scale turbulent eddies that suppress the electron transport. After Shaikh and Shukla (2008).

state, nonlinearly coupled EPOs form stationary structures, and D_{eff} saturates eventually. Thus, remarkably an enhanced electron diffusion results primarily due to the emergence of large-scale potential structures in our 3D quantum plasma.

VII. NONLINEARLY COUPLED ELECTROMAGNETIC AND ELECTROSTATIC WAVES

We turn our attention to the nonlinear interactions between large amplitude electromagnetic and electrostatic waves in dense quantum plasmas. Shukla and Stenflo (2006) considered nonlinear couplings between the large amplitude electromagnetic waves and finite amplitude electron and ion plasma waves, and presented nonlinear dispersion relations that exhibit stimulated Raman scattering (SRS), stimulated Brillouin scattering (SBS), and modulational instabilities. The work of Shukla and Stenflo (Shukla and Stenflo, 2006) has been further generalized by including thermal corrections to electrostatic waves (Stenflo and Shukla, 2009) and relativistic electron mass variations (Shukla and Eliasson, 2007) caused by electromagnetic waves in quantum plasmas.

A. Stimulated Scattering Instabilities

First, we present the governing equations for the high-frequency electromagnetic waves and the electromagnetic wave pressure driven modified Langmuir and ion-acoustic

oscillations. We have (Stenflo and Shukla, 2009)

$$\left(\frac{\partial^2}{\partial t^2} - c^2 \nabla^2 + \omega_{pe}^2 \right) \mathbf{A} + \omega_{pe}^2 \frac{n_1}{n_0} \mathbf{A} \approx 0, \quad (90)$$

for the light wave,

$$\left(\frac{\partial^2}{\partial t^2} + \omega_{pe}^2 - \frac{3}{5} V_{Fe}^2 \nabla^2 + \frac{\hbar^2}{4m_e^2} \nabla^4 \right) \frac{n_1}{n_0} = \frac{e^2}{2m_e^2 c^2} \nabla |\mathbf{A}|^2, \quad (91)$$

for the electromagnetic wave pressure driven electron plasma waves, and

$$\left(\frac{\partial^2}{\partial t^2} - C_{TF}^2 \nabla^2 + \frac{\hbar^2}{4m_e m_i} \nabla^4 \right) \frac{n_1}{n_0} = \frac{e^2}{2m_e m_i c^2} \nabla |\mathbf{A}|^2, \quad (92)$$

for the light pressure driven modified ion-acoustic waves. Here $C_{TF} = (k_B T_{Fe} / m_i)^{1/2}$ and $n_1 (\ll n_0)$ is a small perturbation in the electron number density.

Following the standard procedure of the parametric instabilities (Murtaza and Shukla, 1984; Sharma and Shukla, 1983; Shukla, 2006; Shukla and Eliasson, 2006; Shukla *et al.*, 1981; Yu *et al.*, 1974), we can Fourier analyze (90)-(92) and combine the resultant equations to obtain the nonlinear dispersion relations

$$\omega^2 - \Omega_R^2 = - \frac{e^2 \omega_{pe}^2 k^2 |\mathbf{A}_0|^2}{2m_e^2 c^2} \sum_{+,-} \frac{1}{D_{+,-}}, \quad (93)$$

and

$$\omega^2 - \Omega_B^2 = \frac{e^2 \omega_{pe}^2 k^2 |\mathbf{A}_0|^2}{2m_e m_i c^2} \sum_{+,-} \frac{1}{D_{+,-}}, \quad (94)$$

which admit SRS, SBS, and modulational instabilities of the electromagnetic pump (with the amplitude \mathbf{A}_0) in dense quantum plasmas. We have denoted $D_{+,i} = \pm 2\omega_0(\omega - \mathbf{k} \cdot \mathbf{V}_g \mp \delta)$, where $\mathbf{V}_g = \mathbf{k}c^2/2\omega_0$ is the group velocity of the pump wave with the frequency $\omega_0 = k_0^2 c^2 + \omega_{pe}^2)^{1/2}$ and $\delta = k^2 c^2 / 2\omega_0$ is a nonlinear frequency shift, and

$$\Omega_R^2 = \omega_{pe}^2 + \frac{3}{5} k^2 V_{TF}^2 + \frac{\hbar^2 k^4}{4m_e^2}, \quad (95)$$

and

$$\Omega_B^2 = k^2 C_{TF}^2 + \frac{\hbar^2 k^4}{4m_e m_i}. \quad (96)$$

The growth rates of SRS and SBS instabilities (Shukla and Stenflo, 2006) are, respectively,

$$\gamma_R = \frac{\omega_{pe} e K |\mathbf{A}_0|}{2\sqrt{2}\omega_0 \Omega_R m_e c}, \quad (97)$$

and

$$\gamma_B = \frac{\omega_{pe} e K |\mathbf{A}_0|}{2\sqrt{2}\omega_0 \Omega_B m_e m_i c}. \quad (98)$$

The present results of SRS and SBS instabilities will help to identify the electrostatic spectral lines that are enhanced by the large amplitude electromagnetic pump wave in dense quantum plasmas.

B. Nonlinearly Coupled Intense EM and EPOs

Here we consider nonlinear interactions between an arbitrary large amplitude circularly polarized electromagnetic (CPEM) wave and nonlinear EPOs that are driven by the relativistic ponderomotive force (Shukla and Yu, 1984; Shukla *et al.*, 1985) of the CPEM waves. Such an interaction gives rise to an envelope of the CPEM vector potential $\mathbf{A}_\perp = A_\perp(\hat{\mathbf{x}} + i\hat{\mathbf{y}})\exp(-i\omega_0 t + ik_0 z)$, which obeys the nonlinear Schrödinger equation (Shukla and Eliasson, 2007)

$$2i\epsilon \left(\frac{\partial}{\partial t} + U_g \frac{\partial}{\partial z} \right) A_\perp + \frac{\partial^2 A_\perp}{\partial z^2} - \left(\frac{|\psi|^2}{\gamma} - 1 \right) A_\perp = 0, \quad (99)$$

where $\epsilon = \omega_0/\omega_{pe}$, and the normalized (by $\sqrt{n_0}$) electron wave function ψ and the normalized (by $m_0 c^2/e$) scalar potential are governed by, respectively,

$$iH_e \frac{\partial \psi}{\partial t} + \frac{H_e^2}{2} \frac{\partial^2 \psi}{\partial z^2} + (\phi - \gamma + 1)\psi = 0, \quad (100)$$

and

$$\frac{\partial^2 \phi}{\partial z^2} = |\psi|^2 - 1, \quad (101)$$

where m_0 is the rest mass of the electrons, $U_g = k_0 c/2\omega_0$, $H_e = \hbar\omega_{pe}/m_0 c^2$ is the ration between the plasmonic energy density to the rest electron energy, and $\gamma = (1 + |A_\perp|^2)^{1/2}$ is the relativistic gamma factor due to the electron quiver velocity in the CPEM wave fields. The time and space variables are in units of the electron plasma period (ω_{pe}^{-1}) and the electron skin depth $\lambda_e = c/\omega_{pe}$. The electron density and A_\perp are in units of n_0 and $m_0 c^2/e$ Shukla and Eliasson (2007). The nonlinear coupling between intense CPEM waves and EPOs comes about due to the nonlinear current density, which is represented by the term $|\psi|^2 A_\perp/\gamma$ in Eq. (99). In Eq. (100), $1 - \gamma$ is the relativistic ponderomotive potential (Shukla and Yu, 1984; Shukla *et al.*, 1985). The latter arises from the averaging (over the CPEM wave period $2\pi/\omega_0$) of the relativistic advection and the nonlinear Lorentz force involving the electron quiver velocity and the CPEM wave electric and magnetic fields.

A relativistically strong EM wave in a classical electron-ion plasma is subject to SRS and modulational instabilities (McKinstrie and Bingham, 1992). One can expect that these instabilities will be modified at quantum scale by the dispersion effects caused by the tunneling of electrons through the quantum Bohm potential. The growth rate of the relativistic parametric instabilities in a dense quantum plasma in the presence of a relativistically strong CPEM pump wave can be obtained in a standard manner (Shukla *et al.*, 1985) by letting $\phi(z, t) = \phi_1(z, t)$, $A_\perp(z, t) = [A_0 + A_1(z, t)]\exp(-i\alpha_0 t)$ and $\psi(z, t) = [1 + \psi_1(z, t)]\exp(-i\beta_0 t)$, where A_0 is the large-amplitude CPEM pump and A_1 is the small-amplitude perturbation of the CPEM wave amplitude due to the nonlinear coupling between the CPEM waves

and EPOs, i.e. $|A_1| \ll |A_0|$, and $\psi_1 (\ll 1)$ is the small-amplitude perturbation in the electron wave function. The constants α_0 and β_0 are constant frequency shifts, determined from Eqs. (99) and (100) to be $\alpha_0 = (1/\gamma_0 - 1)/(2\epsilon)$, and $\beta_0 = (1 - \gamma_0)/H_e$, where $\gamma_0 = (1 + |A_0|^2)^{1/2}$. The first-order perturbations in the electromagnetic vector potential and the electron wave function are expanded into their respective sidebands as $A_1(z, t) = A_+ \exp(iKz - i\Omega t) + A_- \exp(-iKz + i\Omega t)$ and $\psi_1(z, t) = \psi_+ \exp(iKz - i\Omega t) + \psi_- \exp(-iKz + i\Omega t)$, while the potential is expanded as $\phi(z, t) = \hat{\phi} \exp(iKz - i\Omega t) + \hat{\phi}^* \exp(-iKz + i\Omega t)$, where Ω and K are the normalized frequency and the normalized wave number of the EPOs, respectively. Inserting the above mentioned Fourier ansatz into Eqs. (99)–(101), linearizing the resultant system of equations, and sorting into equations for different Fourier modes, one obtains the nonlinear dispersion relation (Shukla and Eliasson, 2007)

$$1 - \left(\frac{1}{D_+} + \frac{1}{D_-} \right) \left(1 + \frac{K^2}{D_L} \right) \frac{|A_0|^2}{2\gamma_0^3} = 0, \quad (102)$$

where $D_\pm = \mp 2\Omega_0(\Omega - KU_g) + K^2$ and $D_L = 1 - \epsilon^2 + H_e^2 K^4/4$. We note that $D_L = 0$ yields the linear dispersion relation $\Omega^2 = 1 + H_e^2 K^4/4$ for the EPOs in a dense quantum plasma (Pines, 1961). For $H_e \rightarrow 0$ we recover from (102) the nonlinear dispersion relation for relativistically large amplitude EM waves in a classical electron plasma (McKinstrie and Bingham, 1992). The dispersion relation (102) governs stimulated Raman backward and forward scattering instabilities, as well as the modulational instability. In the long wavelength limit $U_g \ll 1$, $\epsilon \approx 1$ one can use the ansatz $\Omega = i\Gamma$, where the normalized (by ω_{pe}) growth rate $\Gamma \ll 1$, and obtain from Eq. (102) the growth rate $\Gamma = (1/2)|K|\{(|A_0|^2/\gamma_0^3)[1 + K^2/(1 + H_e^2 K^4/4)] - K^2\}^{1/2}$ of the modulational instability. For $|K| < 1$ and $H_e < 1$, the linear growth rate is only weakly depending on the quantum parameter H_e .

The quantum dispersion effects on nonlinearly coupled CPEM and EPOs can be studied by considering a steady state structure moving with a constant speed U_g . Inserting the ansatz $A_\perp = W(\xi)\exp(-i\Omega_e t)$, $\psi = P(\xi)\exp(ik_e x - i\omega_e t)$ and $\phi = \phi(\xi)$ into Eqs. (99)–(101), where $\xi = z - U_g t$, $k_e = U_g/H_e$ and $\omega_e = U_g^2/2H_e$, and where $W(\xi)$ and $P(\xi)$ are real, one obtains from (99)–(101) the coupled system of equations (Shukla and Eliasson, 2007)

$$\frac{\partial^2 W}{\partial \xi^2} + \left(\lambda - \frac{P^2}{\gamma} + 1 \right) W = 0, \quad (103)$$

$$\frac{H_e^2}{2} \frac{\partial^2 P}{\partial \xi^2} + (\phi - \gamma + 1)P = 0, \quad (104)$$

where $\gamma = (1 + W^2)^{1/2}$, and

$$\frac{\partial^2 \phi}{\partial \xi^2} = P^2 - 1, \quad (105)$$

with the boundary conditions $W = \Phi = 0$ and $P^2 = 1$ at $|\xi| = \infty$. In Eq. (103), $\lambda = 2\epsilon\Omega_e$ represents a nonlinear frequency shift of the CPEM wave. In the limit $H_e \rightarrow 0$, one has from (104) $\phi = \gamma - 1$, where $P \neq 0$, and one recovers the classical (non-quantum) case of the relativistic solitary waves in a cold plasma (Marburger and Tooper, 1972).

The system of equations (103)–(105) admits a Hamiltonian

$$Q_H = \frac{1}{2} \left(\frac{\partial W}{\partial \xi} \right)^2 + \frac{H_e^2}{2} \left(\frac{\partial P}{\partial \xi} \right)^2 - \frac{1}{2} \left(\frac{\partial \phi}{\partial \xi} \right)^2 + \frac{1}{2} (\lambda + 1)W^2 + P^2 - \gamma P^2 + \phi P^2 - \phi = 0, \quad (106)$$

where the boundary conditions $\partial/\partial\xi = 0$, $W = \phi = 0$ and $|P| = 1$ at $|\xi| = \infty$ have been used.

Numerical solutions of the quasi-stationary system (103)–(105) are presented in Figs. 10 and 11, while time-dependent solutions of Eqs. (99)–(101) are displayed in Figs. 12 and 13. Here parameters were used that are representative of the next generation laser-based plasma compression (LBPC) schemes (Azechi *et al.*, 2006; Malkin *et al.*, 2007). The formula (Shukla *et al.*, 1985) $eA_\perp/mc^2 = 6 \times 10^{-10} \lambda_s \sqrt{I}$ will determine the normalized vector potential, provided that the CPEM wavelength λ_s (in microns) and the CPEM wave intensity I (in W/cm²) are known. It is expected that in LBPC schemes, the electron number density n_0 may reach 10^{27} cm⁻³ and beyond, and the peak values of eA_\perp/mc^2 may be in the range 1-2 (e.g. for focused EM pulses with $\lambda_s \sim 0.15$ nm and $I \sim 5 \times 10^{27}$ W/cm²). For $\omega_{pe} = 1.76 \times 10^{18}$ s⁻¹, one has $\hbar\omega_{pe} = 1.76 \times 10^{-9}$ erg and $H_e = 0.002$, since $mc^2 = 8.1 \times 10^{-7}$ erg. The electron skin depth $\lambda_e \sim 1.7$ Å. On the other hand, a higher value of $H_e = 0.007$ is achieved for $\omega_{pe} = 5.64 \times 10^{18}$ s⁻¹. Thus, our numerical solutions below, based on these two values of H_e , have focused on scenarios that are relevant for the next generation intense laser-solid density plasma interaction experiments (Malkin *et al.*, 2007).

Figures 10 and 11 exhibit numerical solutions of Eqs. (103)–(105) for $H_e = 0.002$ and $H_e = 0.007$. The nonlinear boundary value problem was solved with the boundary conditions $W = \phi = 0$ and $P = 1$ at the boundaries at $\xi = \pm 10$. We see that the solitary envelope pulse is composed of a single maximum of the localized vector potential W and a local depletion of the electron density P^2 , and a localized positive potential ϕ at the center of the solitary pulse. The latter has a continuous spectrum in λ , where larger values of negative λ are associated with larger amplitude solitary EM pulses. At the center of the solitary EM pulse, the electron density is partially depleted, as in panels a) of Fig. 10, and for larger amplitudes of the EM waves one has a stronger depletion of the electron density, as shown in panels b) and c) of Fig. 10. For cases where the electron density goes to almost zero in the classical case (Marburger and Tooper, 1972), one important quantum effect is that the electrons can tunnel through the depleted density region. This is seen

in Fig. 11, where the electron density remains nonzero for $H_e = 0.007$ in panels a), while the density shrinks to zero for $H_e = 0.002$ in panel b).

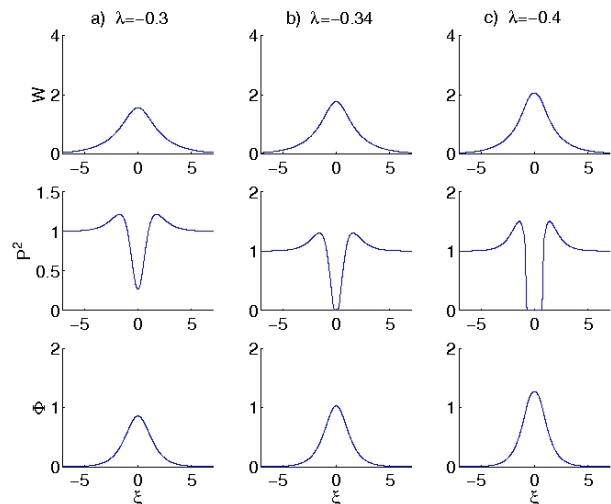


FIG. 10 The profiles of the CPEM vector potential W (top row), the electron number density P^2 (middle row) and the scalar potential Φ (bottom row) for $\lambda = -0.3$ (left column), $\lambda = -0.34$ (middle column) and $\lambda = -0.4$ (right column), with $H_e = 0.002$. After Shukla and Eliasson (2007).

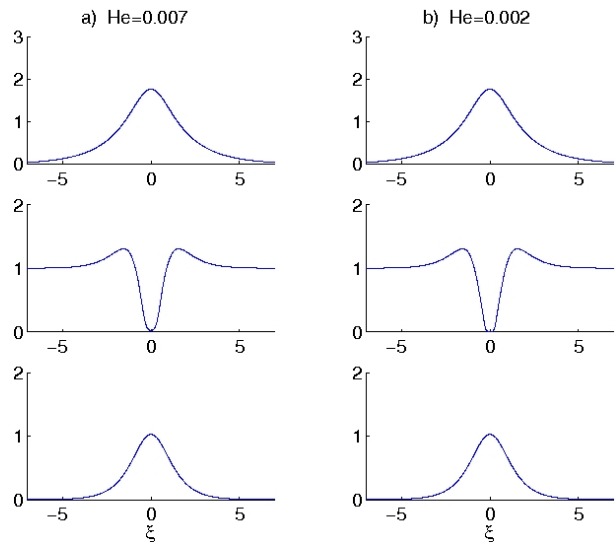


FIG. 11 The profiles of the CPEM vector potential W (top row), the electron number density P^2 (middle row) and the scalar potential Φ (bottom row) for $H_e = 0.007$ (left column) and $H_e = 0.002$ (right column), with $\lambda = -0.34$. After Shukla and Eliasson (2007).

Figures 12 and 13 depict numerical simulation results of Eqs. (99)–(101) for the long-wavelength limit characterized by $\omega_0 \approx 1$ and $V_g \approx 0$. As initial conditions, we used an EM pump with a constant amplitude $A_\perp = A_0 = 1$ and a uniform plasma density $\psi = 1$, together with a small amplitude noise (random numbers)

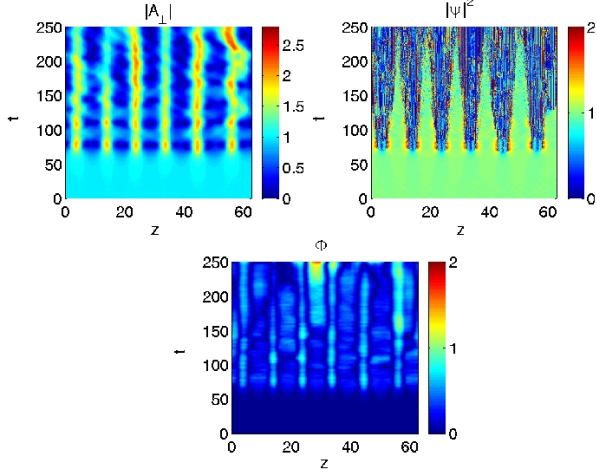


FIG. 12 The dynamics of the CPEM vector potential A_\perp and the electron number density $|\psi|^2$ (upper panels) and of the electrostatic potential Φ (lower panel) for $H_e = 0.002$. After Shukla and Eliasson (2007).

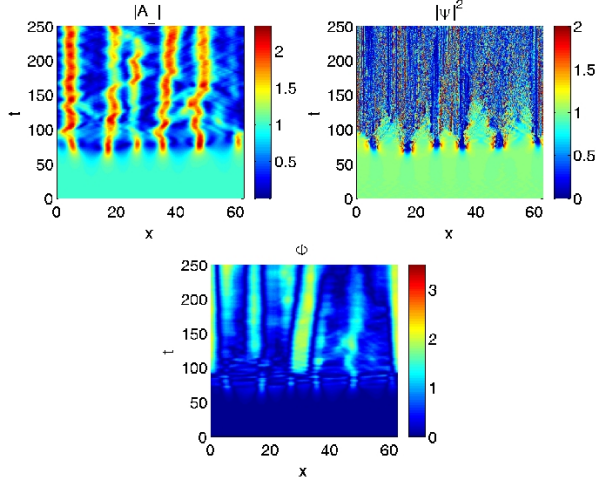


FIG. 13 The dynamics of the CPEM vector potential A_\perp and the electron number density $|\psi|^2$ (upper panels) and the electrostatic potential ϕ (lower panel) for $H_e = 0.007$. After Shukla and Eliasson (2007).

of order 10^{-2} added to A_\perp to give a seeding any instability. The numerical results are displayed in Figs. 12 and 13 for $H_e = 0.002$ and $H_e = 0.007$, respectively. In both cases, we see an initial linear growth phase and a wave collapse at $t \approx 70$, in which almost all the CPEM wave energy is contracted into a few well separated localized CPEM wave pipes. These are characterized by a large bell-shaped amplitude of the CPEM wave, an almost complete depletion of the electron density at the center of the CPEM wavepacket, and a large-amplitude positive electrostatic potential. Comparing Fig. 12 with Fig. 13, we note that there is a more complex dynamics of localized CPEM wavepackets for $H_e = 0.007$, shown in Fig. 13, in comparison with $H_e = 0.002$, shown in Fig.

12, where the wavepackets are almost stationary when they are fully developed.

VIII. DENSE MAGNETIZED PLASMAS

Dense magnetized plasmas occur in the core of white dwarf stars and on the surface of magnetized stars (e.g. magnetars) where degenerate electrons could be ultra-relativistic, but the ions are in a non-degenerate state. How strong magnetic fields in dense stars come about is still a mystery, although there are evidence of the strong magnetization of dense plasmas in astrophysical environments. In dense magnetized plasmas, one has to account for the Lorentz force and the Landau quantization effect (Landau and Lifshitz, 1998a), and develop the appropriate quantum Hall-magnetohydrodynamics (Q-HMHD) equations starting from the Wigner-Maxwell equations.

A. Landau Quantization

In a strong magnetic field $\hat{z}B_0$, where \hat{z} is the unit vector along the z -axis in a Cartesian coordinate system, and B_0 the strength of the external magnetic field, the electron motion in a plane perpendicular to the magnetic field direction is quantized (Landau and Lifshitz, 1998b). The electron energy level is determined by the non-relativistic limit by the expression (Landau and Lifshitz, 1998b; Tsintsadze, 2009)

$$\mathcal{E}_e^{l,\sigma} = \frac{p_z^2}{2m_e} + (2l + 1 + \sigma)\mu_B B_0, \quad (107)$$

where p_z is the electron momentum in the z -direction, l the orbital angular number ($l = 0, 1, 2$), and $\sigma = \pm 1$ represents the spin orientation. For $\sigma = -1$, we have from

$$\mathcal{E}_e^l = \frac{p_z^2}{2m_e} + l\hbar\omega_{ce}, \quad (108)$$

where $\omega_{ce} = eB_0/m_e c$ is the electron gyrofrequency. Accordingly, the Fermi-Dirac electron distribution is (Tsintsadze, 2009)

$$F_D(p_z, l) \propto \frac{1}{1 + \exp[(E_z + l\hbar\omega_{ce} - \mu_e)/k_B T_{Fe}]}, \quad (109)$$

where $E_z = (m_e/2)v_z^2$ is the parallel (to \hat{z}) kinetic energy of the degenerate electrons.

Assuming that $|l\omega_{ce} - \mu_e| \gg k_B T_{Fe}$, one can approximate the Fermi-Dirac distribution function by the Heaviside step function $H(\mu_e - \mathcal{E}_e^l)$, which equal 1 for $\mu_e = E_{Fe} = k_B T_{Fe} = (p_F^2/2m_e)^{1/2} > \mathcal{E}_e^l$ and zero for $E_{Fe} < \mathcal{E}_e^l$, where $p_F = m_e v_{TF}$. The equilibrium electron number density is (Tsintsadze, 2009)

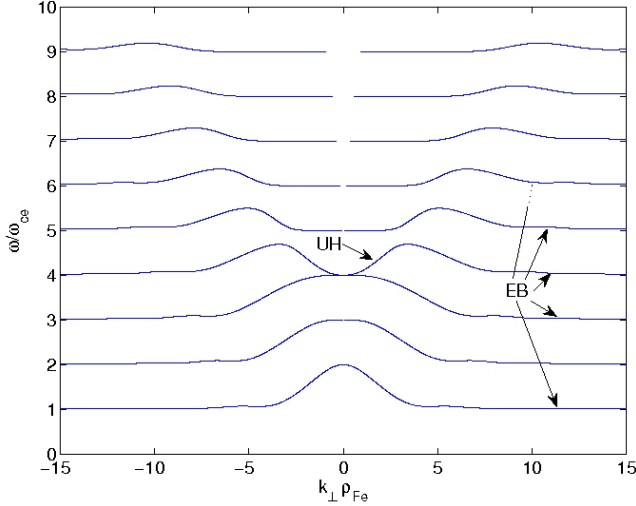


FIG. 14 Dispersion curves for EB waves in a Fermi-Dirac distributed plasma, showing several EB modes and the UH cutoff. After Eliasson and Shukla (2008b).

$$n_e = \frac{p_F^3}{2\pi^2 \hbar^3} \left[\Gamma_B + \frac{2}{3}(1 - \Gamma_B)^{3/2} \right], \quad (110)$$

where $\Gamma_B = \hbar\omega_{ce}/k_B T_{Fe}$.

B. ESOs and EM Waves

In magnetized quantum plasmas, there are finite density perturbations associated with high-frequency electrostatic electron-Bernstein (EB) waves and elliptically polarized EM waves (EP-EM waves) that propagate across the magnetic field direction $\hat{\mathbf{z}}$. Furthermore, the circularly polarized electromagnetic (CPEM) wave propagating along $\hat{\mathbf{z}}$ are not associated with any density perturbation.

The dispersion relation for the EB waves in a Fermi-Dirac distributed plasma is (Eliasson and Shukla, 2008b)

$$1 + \frac{3\omega_{pe}^2}{\omega_{ce}^2} \int_0^\pi d\theta \frac{\sin(\Omega\theta) \sin(\theta) \sin(\xi_e) - \xi_e \cos(\xi_e)}{\xi_e^3} = 0, \quad (111)$$

where $\Omega = \omega/\omega_{ce}$, $\xi_e = (2k_{\perp}^2 \rho_{Fe}^2) \cos(\theta/2)$, and $\rho_{Fe} = V_{Fe}/\omega_{pe}$ is the thermal gyroradius of the degenerate electrons. Solutions of Eq. (111) are plotted in Fig. 14 for the case $\omega_{UH} = 4\omega_{ce}$, where $\omega_{UH} = (\omega_{pe}^2 + \omega_{ce}^2)^{1/2}$ is the upper-hybrid (UH) resonance frequency. In the long wavelength limit (viz. $k_{\perp}^2 \rho_{Fe}^2 \ll 1$), (111) yields

$$\omega^2 = \omega_{UH}^2 + \frac{3}{5} \frac{\omega_{pe}^2 k_{\perp}^2 V_{Fe}^2}{(\omega^2 - 4\omega_{ce}^2)}, \quad (112)$$

where k_{\perp} is the perpendicular (to $\hat{\mathbf{z}}$ component of the propagation wave vector. For $\omega \approx \omega_H$, Eq. (112) reveals

that the propagating UH waves have positive (negative) group dispersion in plasmas with $\omega_{pe} > (<) \sqrt{3}\omega_{ce}$.

Furthermore, the refractive index N_x for the EP-EM waves propagating along the x axis (which is orthogonal to $\hat{\mathbf{z}}$) is (Shukla, 2007)

$$N_x = \frac{k_x^2 c^2}{\omega^2} = 1 - \frac{\omega_{pe}^2}{\omega^2} - \frac{\omega_{pe}^2 \omega_{ce}^2 [1 + \eta(\alpha) k_x^2 \lambda_b^2]}{\omega^2 [\omega^2 - \omega_{UH}^2 + k_x^2 V_{Fe}^2 (1 + k_x^2 \lambda_q^2)]}, \quad (113)$$

where k_x is the x component of the propagation wave vector, $\lambda_q = \hbar^2/4m_e V_{Fe}^2$, $\lambda_b = \sqrt{\hbar/2m_e \omega_{ce}}$, $\eta(\alpha) = 2 \tanh(\alpha)$, $\alpha = \mu_B B_0/k_B T_{Fe}$. Several comments are in order. First, we note that the electron 1/2- spin effect enhances the electron gyrofrequency by a factor $(1 + \eta k_x^2 \lambda_b^2)^{1/2}$ in the numerator of the third term in the right-hand side of (113). Second, the quantum Bohm force produces a dispersion term $\hbar k^4/4m_e^2$ in the denominator of the third term in (113). Third, in the limit of vanishing \hbar , Eq. (113) correctly reproduces the EP-EM wave dispersion relation. Furthermore, Eq. (113) reveals that the cut-off frequencies (at $k_x = 0$) in dense magnetoplasmas are

$$\omega = \omega_{\pm} = \frac{1}{2} \left[(4\omega_{pe}^2 + \omega_{ce}^2)^{1/2} \pm \omega_{ce} \right], \quad (114)$$

which are the same as the cutoffs of the X (upper sign) and Z (lower sign) mode waves in a classical plasma (Chen, 2006).

The vector representation of spinning quantum particles in the quantum theory was first introduced by Takabayashi (1955) who developed the QHD involving the evolution of the quantum particle spin. The idea of Takabayashi has been further elaborated by Brodin *et al.* (2010) in the context of the spin contribution to the ponderomotive force of the magnetic field-aligned CPEM waves in a quantum magnetoplasma. In fact, by using the non-relativistic electron momentum equation (Brodin *et al.*, 2010)

$$m_e \left(\frac{\partial}{\partial t} + \mathbf{u}_e \cdot \nabla \right) \mathbf{u}_e = -e \left(\mathbf{E} + \frac{1}{c} \mathbf{u}_e \times \mathbf{B} \right) - \frac{g}{\hbar} \mu_B \nabla(\mathbf{B} \cdot \mathbf{s}), \quad (115)$$

and the spin evolution equation

$$\left(\frac{\partial}{\partial t} + \mathbf{u}_e \cdot \nabla \right) \mathbf{s} = \frac{g\mu_B}{\hbar} (\mathbf{B} \times \mathbf{s}), \quad (116)$$

together with Ampère's law and suitable Maxwell's equation (incorporating the electron magnetization current, $\mathbf{J}_M = -(4\pi/c)(g\mu_B/\hbar)\nabla \times (n_e \times \mathbf{s})$, due to the electron 1/2- spin effect), where $g = 2.0023192$ is the electron Gaunt factor and \mathbf{s} is the spin angular momentum, with its absolute value $|\mathbf{s}| = s_0 = \hbar/2$, Brodin *et al.* derived the spin ponderomotive force $\hat{\mathbf{z}}F_s$ for the CPEM wave. Here we have denoted

$$F_s = \mp \frac{g^2 \mu_B^2}{m_e^2 \hbar^2} \frac{s_0}{(\omega \pm \omega_g)} \left[\frac{\partial}{\partial z} - \frac{k}{(\omega \pm \omega_g)} \frac{\partial}{\partial t} \right] |\mathbf{B}_w|^2, \quad (117)$$

where $\omega_g = g\mu_B B_0/\hbar$ the spin-precession frequency, and \mathbf{B}_w is the CPEM wave magnetic field. The spin ponderomotive force comes from the averaging of the third term in (115) over the CPEM wave period $2\pi/\omega$. The CPEM wave frequency ω is determined from the dispersion relation

$$\left[1 \mp \frac{\omega_\mu}{(\omega \pm \omega_g)}\right] N_z^2 = 1 - \frac{\omega_{pe}^2}{\omega(\omega \pm \omega_{ce})}, \quad (118)$$

where $N_z = k_z c/\omega$, k_z is the component of the wave vector \mathbf{k} along the z axis, $\omega_\mu = g^2 s_0/4m_e \lambda_e^2$, $\lambda_e = c/\omega_{pe}$, and the $+$ ($-$) represents the left- (right-) hand circular polarization. The ω_μ -term in (117) is associated with the electron spin evolution. It changes the dispersion properties of the magnetic field-aligned EM electron-cyclotron waves in dense magnetoplasmas. Furthermore, the spin-ponderomotive force induces a strong spin-polarization of the dense quantum magnetoplasma.

It should be noted that there is also a standard non-stationary ponderomotive force ($\hat{\mathbf{z}}F_e$) (Karpman and Washimi, 1977) of the CPEM waves arising from the averaging of the nonlinear Lorentz force term $-(e/m_e c)\hat{\mathbf{z}} \cdot (\mathbf{u}_e \times \mathbf{B}_w)$ over the CPEM wave $2\pi/\omega$ in our quantum plasma, where

$$F_e = -\frac{e^2}{2m_e^2 \omega(\omega \pm \omega_{ce})} \left[\frac{\partial}{\partial z} \pm \frac{k_z \omega_{ce}}{\omega(\omega \pm \omega_{ce})} \frac{\partial}{\partial t} \right] |\mathbf{E}_w|^2, \quad (119)$$

where $\mathbf{E}_w = (\omega/k_z c)\mathbf{B}_w$ is the CPEM wave electric field.

C. Q-HMHD Equations

To a first approximation, the dynamics of low phase speed (in comparison with the speed of light in vacuum) electromagnetic waves in dense magnetoplasmas is modeled by the Q-HMHD equations. The latter include the inertialess electron momentum equation

$$0 = -en_e \left(\mathbf{E} + \frac{1}{c} \mathbf{u}_e \times \mathbf{B} \right) - \nabla P_C, \quad (120)$$

where the quantum Bohm and quantum spin forces are supposed to be unimportant on the characteristic scale-length of our interest. The degenerate electrons are coupled with the non-degenerate ions through the electromagnetic forces. The ion dynamics is governed by the ion continuity equation (61) and the momentum equation

$$m_i n_i \frac{d\mathbf{u}_i}{dt} = n_i e \left(\mathbf{E} + \frac{1}{c} \mathbf{u}_i \times \mathbf{B} \right), \quad (121)$$

where $d/dt = (\partial/\partial t) + \mathbf{u}_i \cdot \nabla$. The electromagnetic fields are given by Ampère's law

$$\frac{\partial \mathbf{B}}{\partial t} = -c \nabla \times \mathbf{E}, \quad (122)$$

and Maxwell's equation

$$\nabla \times \mathbf{B} = \frac{4\pi e}{c} (n_i \mathbf{u}_i - n_e \mathbf{u}_i) + \frac{1}{c} \frac{\partial \mathbf{E}}{\partial t}. \quad (123)$$

By using (120), we can eliminate the electric field \mathbf{E} from (121), obtaining for a quasi-neutral ($n_e = n_i = n$) dense magnetoplasma

$$m_i n \frac{d\mathbf{u}_i}{dt} = -\nabla P_C - \frac{1}{8\pi} \nabla \mathbf{B}^2 + \frac{(\mathbf{B} \cdot \nabla) \mathbf{B}}{4\pi}, \quad (124)$$

where we have used (123) without the displacement current for the low-phase speed (in comparison with c) EM wave phenomena. By using the electric field from (121), we can write (122) as

$$\frac{\partial \mathbf{B}}{\partial t} = \nabla \times (\mathbf{u}_i \times \mathbf{B}) - \frac{m_i c}{e} \frac{d\mathbf{u}_i}{dt}, \quad (125)$$

Equations (61), (124) and (125) are the desired Q-HMHD equations for studying the linear and nonlinear dispersive electromagnetic waves, as well as new aspects of 3D quantum fluid turbulence in a dense quantum magnetoplasma with degenerate electrons having Chandrasekhar's pressure law. However, when the Landau quantization effect in a very strong magnetic field is accounted for, one can replace P_C by the appropriate pressure law (Eliezer *et al.*, 2005)

$$P_L = \frac{4eB_0(2m_e)^{1/2} E_F^{3/2}}{3(2\pi)^2 \hbar^2 c} \left[1 + 2 \sum_{l=1}^{l_m} \left(1 - \frac{l\hbar\omega_{ce}}{k_B T_{Fe}} \right)^{3/2} \right], \quad (126)$$

where the value of l_m is fixed by the largest integer that satisfies $k_B T_{Fe} - l\hbar\omega_{ce} \leq 0$.

IX. SUMMARY AND OUTLOOK

In this Colloquium paper, we have described the essential physics of dense quantum plasmas with degenerate electrons. We have reviewed the properties of quantum plasmas and quantum models that describe the essential features of linear and nonlinear electrostatic and electromagnetic waves. Specifically, the focus of the present colloquium article has been on the model nonlinear equations that depict new features of quantum nonlinear waves and quantum electron fluid turbulence at nanoscales. Numerical simulations of the nonlinear Schrödinger (NLS)-Poisson equations reveal quasi-stationary, localized structures in the form of one-dimensional electron density holes (dark solitons) and

two-dimensional quantum electron vortices. These localized quantum structures are associated with a local depletion of the electron density associated with a positive electrostatic potential. In the two-dimensional space dimension, there exist a class of quantum electron vortices of different excited states (charge states). Furthermore, numerical simulations also depict that the time-dependent NLS-Poisson equations exhibit stability of a dark soliton in one-space dimension. In two-space dimensions, the dark solitons of the first excited state are stable and the preferred nonlinear state is in the form of quantum vortex pairs of different polarities. The one-dimensional dark soliton and singly charged two-dimensional quantum vortices are thus long-lived nonlinear structures. Also presented are theoretical and computer simulation studies of nonlinearly coupled intense EM waves and EPOs in very dense quantum plasmas. We have reported new classes of stimulated scattering instabilities of EM waves and trapping of intense EM waves in a quantum electron density hole.

It should be that inclusion of the non-degenerate ion dynamics gives rise to new features to the nonlinear electrostatic waves (Eliasson and Shukla, 2008a; Haas *et al.*, 2003), especially to the nonlinear dispersive ion-acoustic waves in an unmagnetized quantum plasma. Furthermore, the nonlinear equations governing the coupling between the dispersive Langmuir and ion-acoustic waves, which are known as the quantum Zakharov equations (Garcia *et al.*, 2005; Haas and Shukla, 2009; Misra *et al.*, 2008; Simpson *et al.*, 2009), admit periodic, quasi-periodic, chaotic and hyper-chaotic states (Misra *et al.*, 2008), in addition to arresting the Langmuir wave collapse (Haas and Shukla, 2009; Simpson *et al.*, 2009) due to quantum effects. There may also emerge new aspects of the nonlinear electron plasma waves when the quantum particle trapping (Jovanovic and Fedele, 2007) in the strong wave potential is included. Here one has to obtain nonlinear solutions of the non-stationary Wigner-Poisson equations, which might reveal a modified (by the electrostatic wave potential) Fermi-Dirac electron distribution function.

The field of the nonlinear quantum plasma physics is vibrant, and its potential applications rest on our complete understanding of numerous collective processes in compact astrophysical objects, as well as in the next-generation of intense laser-solid density plasma experiments and in the plasma assisted nanotechnology (e.g. quantum free electron laser devices, quantum-diodes, metallic nanostructures, nanowires, nanotubes, etc.). However, the nonlinear quantum models presented herein have to be further improved and generalized by including the effects of the electron exchange interactions, strong electron-electron correlations, the equilibrium inhomogeneous magnetic field and the equilibrium electron density gradient, the plasma boundary, as well as fully relativistic Landau quantization of quantum particles. We have also to understand the features of quantum oscillations of electrons and possible formation of bound states of

electrons in the presence of an external magnetic field. For this purpose, we have to calculate the interaction potential among highly correlated electrons and use the molecular dynamic simulations to demonstrate attraction between electrons due to collective wave-quantum particle interactions that give rise to Cooper's pairing of electrons. The Cooper's pairing of electrons could possibly provide a scenario of superconducting behavior of dense quantum plasmas. Moreover, in a nonuniform dense magnetoplasma, we have electrostatic drift waves (Ali *et al.*, 2007; Saleem *et al.*, 2008; Shokri and Rukhadze, 1999) which drastically affect the cross-field electron transport. Furthermore, in the study of nonlinear collective interactions in plasma assisted nano-technology devices (e.g. nonlinear electrostatic and electromagnetic surface waves in metallic nanostructure-devices, photonic band gap and x-ray optical systems, quantum X-ray free-electron laser systems), we have to carefully examine the combined effects of the electron-1/2 spin and quantum electron tunneling. Finally, the localization of electrostatic and electromagnetic waves due to nonlinear quantum effects in a nonuniform dense magnetoplasma with an arbitrary electron pressure degeneracy should provide clues to the origin of very intense X-rays (Coe *et al.*, 1978) and gamma rays (Hurley *et al.*, 2005) from both astrophysical and laboratory plasmas.

Acknowledgments

This research was supported by the Deutsche Forschungsgemeinschaft through the project SH21/3-1 of the Research Unit 1048, and by the Swedish Research Council (VR).

References

- Ali, S., N. Shukla, and P. K. Shukla, 2007, *Europhys. J. Lett.* **78**, 45001.
- Anderson, D., B. Hall, M. Lisak, and M. Marklund, 2002, *Phys. Rev. E* **65**, 046417.
- Andreev, A. V., 2000, *JETP Lett.* **72**, 238.
- Ang, L. K., *et al.*, 2003, *Phys. Rev. Lett.* **91**, 208303.
- Ang, L. K., and P. Zhang, 2007, *Phys. Rev. Lett.* **98**, 164802.
- Atwater, H. A., 2007, *Sci. Am.* **296**, 56.
- Azechi, H., *et al.*, 2006, *Plasma Phys. Control. Fusion* **48**, B267.
- Barnes, W., A. Dereux, and T. Ebbesen, 2003, *Nature (London)* **424**, 824.
- Becker, K. H., K.H. Schoenbach, and J.G. Eden, 2006, *J. Phys. D: Appl. Phys.* **39**, R55.
- Benvenuto O. G., and M. A. De Vito, 2005, *Mon. Not. R. Astron.* **362**, 891.
- Berestetskii, B., E. M. Lifshitz, and L. P. Pitaevskii, 1999, *Quantum Electrodynamics* (Butterworth-Heinemann, Oxford), p. 123.
- Bohm, D., 1953, *Phys. Rev.* **92**, 626.
- Bohm, D., and D. Pines, 1953, *Phys. Rev.* **92**, 609.

- Bonitz, M., 1998, *Quantum Kinetic Theory* (Teubner, Stuttgart).
- Bransden, B. H., and C. J. Joachain, 2000, *Quantum Mechanics (2nd Edition)* (Pearson Education Limited, Essex, England).
- Brodin, G., and M. Marklund, 2007a, *New J. Phys.* **9**, 277.
- Brodin, G., and M. Marklund, 2007b, *Phys. Plasmas* **14**, 11207.
- Brodin, G., and M. Marklund, 2007c, *Phys. Rev. E* **76**, 055403(R).
- Brodin, G., M. Marklund, J. Zamanian, A. Ericsson, and P. L. Mana, 2008, *Phys. Rev. Lett.* **101**, 245002.
- Brodin, G., A. P. Misra, and M. Marklund, 2010, *Phys. Rev. Lett.* **105**, 105004.
- Burt, P., and D. Wahlquist, 1962, *Phys. Rev.* **125**, 1785.
- Chabrier, G., *et al.*, 2002, *J. Phys.: Condens. Matter* **14** 9133.
- Chabrier, G., D. Saumon, and A. Y. Potekhin, 2006, *J. Phys. A: Math. Gen.* **39**, 4411.
- Chabrier, G., 2009, *Plasma Phys. Control. Fusion* **51**, 124014.
- Chandrasekhar, S., 1931, *Astrophys. J.* **74**, 81; *Phil. Mag.* **11**, 592 (1931).
- Chandrasekhar, S., 1935, *Mon. Not. R. Astron. Soc.* **170**, 405.
- Chandrasekhar, S., 1939, *An Introduction to the Study of Stellar Structure* (University of Chicago Press, Chicago), p. 360.
- Chang, D. E., *et al.*, 2006, *Phys. Rev. Lett.* **97**, 053002.
- Chen, F. F., 2006, *Introduction to plasma physics and controlled fusion. Volume 1, Plasma physics*. Second edition (Springer, New York).
- Coe, M. J., A. R. Engel, and J. J. Quenby, 1978, *Nature (London)* **272**, 37.
- Crouseilles, N., P. A. Hervieux, and G. Manfredi, 2008, *Phys. Rev. B* **78**, 155412.
- Dirac, P. A. M., 1981, *Principles of Quantum Mechanics* (Oxford University Press, Oxford).
- Drake, R. P., 2009, *Phys. Plasmas* **16**, 055501; *Phys. Today* **63**, 28 (2010).
- Dvornikov, M., 2009, *Formation of Cooper pairs in quantum oscillations of electrons in plasma*, arXiv:0902.4596v1 [physics.plasm-ph] 26 Feb 2009.
- Eliasson, B., and P. K. Shukla, 2008a, *J. Plasma Phys.* **64**, 581.
- Eliasson, B., and P. K. Shukla, 2008b, *Phys. Plasmas* **15**, 102102.
- Eliezer, S., P. Norreys, J. T. Mendonça, and K. Lancaster, 2005, *Phys. Plasmas* **12**, 052115.
- Else, D., R. Kompaneets, and S. V. Vladimirov, 2010, *Phys. Rev. E* **82**, 026410.
- Fortov, V. E., 2009, *Phys. Usp.* **52**, 615.
- Frisch, U., 1995, *Turbulence* (Cambridge University Press, Cambridge).
- Garcia, L. G., F. Haas, L. P. L. de Oliveira, and J. Goedert, 2005, *Phys. Plasmas* **12**, 012302.
- Gardner, C. L., and C. Ringhofer, 1996, *Phys. Rev. E* **53**, 157.
- Gerritsma, R., G. Kirchmair, F. Zähringer, E. Solano, R. Blatt, and C. F. Roos, 2010, *Nature (London)* **463**, 68.
- Ghoshal, A., and Y. K. Ho, 2009a, *Phys. Rev. A* **79**, 062514.
- Ghoshal, A., and Y. K. Ho, 2009b, *J. Phys. B: At. Mol. Opt. Phys.* **43**, 175006.
- Glenzer, S. H., and R. Redmer, 2009, *Rev. Mod. Phys.* **81**, 1625.
- Glenzer, S. H., *et al.*, 2007, *Phys. Rev. Lett.* **98**, 065002.
- Gottlieb, D., and S. A. Orszag, 1977, *Numerical Analysis of Spectral Methods* (SIAM, Philadelphia).
- Guillot, T., 1999, *Science* **286**, 72.
- Gursky, H., 1976, in *Frontiers of Astrophysics*, Ed. E. H. Avrett (Harvard University Press, Cambridge, Massachusetts), Chap. 5, pp. 152,153.
- Haas, H., 2005, *Phys. Plasmas* **12**, 062117.
- Haas, H., 2007, *Europhys. Lett.* **44**, 45004.
- Haas, F., L. G. Garcia, J. Goedert, and G. Manfredi, 2003, *Phys. Plasmas* **10**, 3858.
- Haas, F., and P. K. Shukla, 2009, *Phys. Rev. E* **79**, 066402.
- Haas, F., M. Marklund, G. Brodin, and J. Zamanian, 2010, *Phys. Lett. A* **374**, 481.
- Hakim, R., and J. Heyvaerts, 1978, *Phys. Rev. A* **18**, 1250.
- Harding, A. K., and D. Lai, 2006, *Rep. Prog. Phys.* **69**, 2631.
- Haug, H., and S. W. Koch, 2004, *Quantum Theory of Optical and Electronic Properties of Semiconductors* (World Scientific, Singapore).
- Hillery, M., *et al.*, 1984, *Phys. Rep.* **106**, 121.
- Hohenberg, P., and W. Kohn, 1964, *Phys. Rev.* **136**, B864.
- Holland, P. R., 1993, *The Quantum Theory of Motion* (Cambridge University Press, Cambridge).
- Horn, H. M., 1991, *Science* **252**, 384.
- Hu, S. X., and C.H. Keitel, 1999, *Phys. Rev. Lett.* **83**, 4709.
- Hurley, K., S. E. Boggs, D. M. Smith *et al.*, 2005, *Nature (London)* **434**.
- Ichimaru, S., 1982, *Rev. Mod. Phys.* **54**, 1107.
- Iroshnikov, P., 1963, *Sov. Astron.* **7** 566.
- Jovanovic, D., and R. Fedele, 2007, *Phys. Lett. A* **364**, 304.
- Jüngel, A., D. Matthes, and J. F. Milisic, 2006, *SIAM* **67**, 46.
- Karpman, V. I., and H. Washimi, 1977, *J. Plasma Phys.* **18**, 173.
- Kelly, D. C., 1964, *Phys. Rev.* **134**, A641.
- Klimontovich, Y. L., and V. P. Silin, 1952a, *Doklady Akad. Nauk. SSSR* **82**, 361.
- Klimontovich, Y. L., and V. P. Silin, 1952b, *Zh. Eksp. Teor. Fiz.* **23**, 151.
- Klimontovich, Y. L., and V. P. Silin, 1961, in *Plasma Physics*, Ed. J. E. Drummond (McGraw Hill, New York), pp. 35-87.
- Koester, D., and G. Chanmugam, 1990, *Rep. Prog. Phys.* **53**, 837.
- Kohn W., and L. J. Sham, 1965, *Phys. Rev.* **140**, A1133.
- Kolmogorov, A. N., 1941, *Dokl. Akad. Nauk SSR* **30** 301; **31** 438 (1941).
- Kraichnan, R. H., 1965, *Phys. Fluids* **8** 1385.
- Kremp, D., Th. Bornath, M. Bonitz, and M. Schlanges, 1999, *Phys. Rev. E* **60**, 4725.
- Kremp, D., M. Schlanges, and W. D. Kraeft, 2005, *Quantum Statistics of Nonideal Plasmas* (Springer, Berlin).
- Kritcher, A. L., P. Neumayer, J. Castor *et al.*, 2008, *Science* **322**, 69.
- Kuzelev, M. V., and A. A. Rukhadze, 1999, *Phys. Usp.* **42**, 603.
- Lai, D., 2001, *Rev. Mod. Phys.* **73**, 629.
- Landau, L. D., and E. M. Lifshitz, 1998a, *Quantum Mechanics* (Butterworth-Heinemann, Oxford).
- Landau, L. D., and E. M. Lifshitz, 1998b *Statistical Physics* (Butterworth-Heinemann, Oxford).
- Lau, Y. Y., *et al.*, 1991, *Phys. Rev. Lett.* **66**, 1446.
- Lee, H. J., P. Neumayer, J. Castor, *et al.*, 2009, *Phys. Rev. Lett.* **102**, 115001.
- Lesieur, M., 1990, *Turbulence in Fluids* (Kluwer, Dordrecht).
- Lifshitz, E. M., and L. P. Pitaevskii, 1981, *Physical Kinetics* (Butterworth-Heinemann, Oxford), pp. 164-165.
- Maafa, N., 1993, *Physica Scripta* **48**, 351.

- Madelung, E., 1926, *Z. Phys.* **40**, 32.
- Maier, S. A., 2007, *Plasmonics* (Springer, New York).
- Malkin, V. M., *et al.*, 2007, *Phys. Rev. E* **75**, 026404.
- Manfredi, G., 2005, *Fields Inst. Commun.* **46**, 263.
- Manfredi, G., and F. Haas, 2001, *Phys. Rev. B* **64**, 075316.
- Manfredi, G., and P.-A. Hervieux, 2007, *Appl. Phys. Lett.* **91**, 061108.
- Marburger, J. H., and R. F. Tooper, 1975, *Phys. Rev. Lett.* **35**, 1001.
- Marklund, M., and P. K. Shukla, 2006, *Rev. Mod. Phys.* **78**, 591.
- Marklund, M., and G. Brodin, 2007, *Phys. Rev. Lett.* **98**, 025001.
- Marklund, M., G. Brodin, L. Stenflo, and C. S. Liu, 2008, *Europhys. Lett.* **84**, 17006.
- Markowich, P. A., *et al.*, 1990, *Semiconductor Equations* (Springer, Berlin).
- McKinstrie, C. J., and R. Bingham, 1992, *Phys. Fluids B* **4**, 2626.
- Melrose, D. B., 2008, *Quantum Plasmadynamics: Unmagnetized Plasmas* (Springer, New York). Lecture Notes Phys. 735.
- Melrose, D. B., and A. Mushtaq, 2009, *Phys. Plasmas* **16**, 094508.
- Mendonça, J. T., 2001, *Theory of Photon Acceleration* (Institute of Physics, Bristol).
- Misra, A. P., 2007, *Phys. Plasmas* **14**, 064501.
- Misra, A. P., D. Ghosh, and A. R. Chowdhury, 2008, *Phys. Lett. A* **372**, 1469.
- Misra, A. P., 2009, *Phys. Plasmas* **16**, 033702.
- Misra, A. P., and S. Samanta, 2010, *Phys. Rev. E* **82**, 037401.
- Moyal, J. E., 1949, *Proc. Cambridge Philos. Soc.* **45**, 99.
- Murtaza, G. M., and P. K. Shukla, 1984, *J. Plasma Phys.* **31**, 423.
- Mushtaq, A., and D. B. Melrose, 2009, *Phys. Plasmas* **16**, 102110.
- Plasma Science: From Fundamental Research to Technological Applications*, National Research Council (National Academic Press, Washington DC, 1995).
- Neumayer, P., C. Fortmann, T. Döpner, *et al.*, 2010, *Phys. Rev. Lett.* **105**, 075003.
- Norreys, P. A., F. N. Beg, Y. Sentoku, *et al.*, 2009, *Phys. Plasmas* **16**, 041002.
- Oberman, C., and A. Ron, 1963, *Phys. Rev.* **130**, 1291.
- Opher, M., *et al.*, 2001, *Phys. Plasmas* **8**, 2454.
- Ozbay, E., 2006, *Science* **311**, 189.
- Pines, D., 1961, *J. Nucl. Energy: Part C: Plasma Phys.* **2**, 5.
- Pines, D., 1983, *Elementary Excitations in Solids* (Benjamin, Massachusetts).
- Pines, D., and P. Nozieres, 1989, *The Theory of Quantum Liquids* (Benjamin, New York).
- Salamin Y. A., *et al.*, 2006, *Phys. Rep.* **427**, 41.
- Saleem, H., A. Ahmad, and S. A. Khan, 2008, *Phys. Plasmas* **15**, 014503.
- Scott R. K., 2007, *Phys. Rev. E* **75** 046301.
- Serbeto, A., J. T. Mendonça, K. H. Tsui, and R. Bonifacio, 2008, *Phys. Plasmas* **15**, 013110).
- Serbeto, A., L. F. Monteiro, K. H. Tsui, and J. T. Mendonça, 2009, *Plasma Phys. Control. Fusion* **51**, 124024.
- Shaikh, D., and P. K. Shukla, 2007, *Phys. Rev. Lett.* **99** 125002.
- Shaikh, D., and P. K. Shukla, 2008, *New J. Phys.* **10** 083007.
- Shapiro, S. L., and S. L. Teukolsky, 1983, *Black Holes, White Dwarfs, and Neutron Stars: The Physics of Compact Objects* (John Wiley & Sons, New York).
- Sharma, R. P., and P. K. Shukla, 1983, *Phys. Fluids* **26**, 83.
- Shukla, P. K., 2006, *Phys. Lett. A* **352**, 242.
- Shukla, P. K., 2007, *Phys. Lett. A* **369**, 312.
- Shukla, P. K., 2009, *Nature Phys.* **5**, 92.
- Shukla, P. K., 2010, *Phys. Lett A* **374**, 2897.
- Shukla, P. K., and B. Eliasson, 2006, *Phys. Rev. Lett.* **96** 245001.
- Shukla, P. K., and B. Eliasson, 2007, *Phys. Rev. Lett.* **99**, 096401.
- Shukla, P. K., and B. Eliasson, 2008a *Phys. Lett. A* **372**, 2897.
- Shukla, P. K., and B. Eliasson, 2008b, *Phys. Rev. Lett.* **100**, 036801.
- Shukla, P. K., and B. Eliasson, 2010, *Phys. Usp.* **53**, 51.
- Shukla, P. K., and L. Stenflo, 2006, *Phys. Plasmas* **13**, 044505.
- Shukla, P. K., and M. Y. Yu, 1984, *Plasma Phys. Contr. Fusion* **26**, 841.
- Shukla, P. K., M. Y. Yu, H. U. Rahman, *et al.*, 1981, *Phys. Rev. A* **23**, 321.
- Shukla, P. K., N. N. Rao, M. Y. Yu, and N. L. Tsintsadze, 1986, *Phys. Rep.* **138**, 1.
- Shokri, B., and A. A. Rukhadze, 1999, *Phys. Plasmas* **6**, 3450.
- Shpatakovskaya, G., 2006, *J. Exp. Teor. Phys.* **102**, 466.
- Silin, V. P., and A. A. Rukhadze, 1961, *Electromagnetic Properties of Plasmas and Plasma-like Media* (Gosatomizdat, Moscow).
- Simpson, G., C. Sulem, and P. L. Sulem, 2009, *Phys. Rev. E* **80**, 056405.
- Son, S., and N. J. Fisch, 2005, *Phys. Rev. Lett.* **95**, 225002.
- Stenflo, L., and P. K. Shukla, 2009, in *From Leonardo to ITER: Nonlinear and Coherence Aspects*, Ed. J. Weiland. (AIP Conf. Proc., Vol **1177**, New York), pp. 4-9.
- Takabayashi, T., 1955, *Prog. Theo. Phys.* **14**, 283.
- Thaller, B., 1992, *Dirac Equation* (Springer, New York).
- Tsintsadze, L. N., 2009, *Quantization of Longitudinal Electric Waves in Plasmas*, arXiv:0911.0133v1 [physics.plasm-ph].
- Tsintsadze, N. L., and L. N. Tsintsadze, 2009, *Europhys. Lett.* **88**, 35001.
- Wigner, E., 1932, *Phys. Rev.* **40**, 749.
- Xia, S. X., W. C. Hua, and G. Feng, 2010, *Chin. Phys. Lett.* **27**, 025204.
- Yu, M. Y., *et al.*, 1974, *Z. Naturforsch* **29a**, 1736.
- Zhu, J., and P. Ji, 2010, *Phys. Rev. E* **81**, 036406.